NASA TECHNICAL NOTE

NASA TN D-2707

NASA TN D-2707

A FIXED-BASE SIMULATOR STUDY OF PILOTED ENTRY INTO THE EARTH'S ATMOSPHERE AT PARABOLIC VELOCITY

by Martin T. Moul and Albert A. Schy

Langley Research Center
Langley Station, Hampton, Va.

NATIONAL AERONAUTICS AND SPACE ADMINISTRATION • WASHINGTON, D. C. • MARCH 1965

NASA TN D-2707

A FIXED-BASE SIMULATOR STUDY OF PILOTED ENTRY INTO THE EARTH'S ATMOSPHERE AT PARABOLIC VELOCITY

By Martin T. Moul and Albert A. Schy

Langley Research Center
Langley Station, Hampton, Va.

NATIONAL AERONAUTICS AND SPACE ADMINISTRATION

For sale by the Office of Technical Services, Department of Commerce,
Washington, D.C. 20230 -- Price $3.00

A FIXED-BASE SIMULATOR STUDY OF PILOTED ENTRY INTO THE EARTH'S ATMOSPHERE AT PARABOLIC VELOCITY

By Martin T. Moul and Albert A. Schy
Langley Research Center

SUMMARY

18213

Pilot control and navigation of a spacecraft during entry into the earth's atmosphere at parabolic velocity were investigated on a fixed-base analog simulator. The simulation included an analog computer, on which a set of six-degree-of-freedom vehicle equations of motion were solved, and a pilot station consisting of vehicle controllers, a display of standard-research-type-flight instruments, an integrated oscilloscope display of guidance and situation data, and an x-y plotter on which trajectory data were recorded. The spacecraft configuration considered was a blunt-face capsule and was trimmed to a constant lift-drag ratio of 0.5 by offsetting the center of gravity from the axis of symmetry. Reaction controls applying moments about all three axes of the vehicle were simulated with which attitude could be controlled by the pilot and automatic or manual damping augmentation could be introduced. With a fixed lift-drag ratio, the spacecraft trajectory was controlled by rolling the vehicle to vary the vertical and sidewise components of lift. Extreme entries in which the pilot task was to achieve either a long or short range, and entries using a minimum of display instrumentation were considered.

With the aid of specialized navigation displays pilots were able to accomplish long-range navigation with or without three-axis damping augmentation. The displays used were an oscilloscope presentation of acceleration and altitude rate for performing high-altitude skips, and a reference-trajectory presentation for terminal guidance. Without damping augmentation the pilot's attention was continuously required in controlling spacecraft attitude, and this condition was rated as being "acceptable for emergency use only." In short-range entries made by using a display of bank angle and quickened acceleration (acceleration signal passed through a lead filter), pilots were able to accomplish the assigned tasks with or without damping augmentation. For entries in which navigation and range were not considerations, pilots could make safe entries with only bank angle and acceleration displays and with pitch damping augmentation only.

In the three types of entries considered, one integrated oscilloscope display of acceleration, altitude rate, and bank angle was utilized for controlling the vehicle, with modifications in the form of removing altitude rate and quickening acceleration being made at times.

Author

INTRODUCTION

One critical phase of manned lunar missions is that of entering the earth's atmosphere, wherein problems of earth capture, acceleration constraints, aerodynamic heating, and vehicle control and navigation must be solved. The solutions, or the establishment of limits, for the first three of these problem areas define a corridor of atmospheric entry conditions through which all acceptable entry trajectories must pass. Limiting conditions for entry are expressed as overshoot and undershoot boundaries (see fig. 1), and in this investigation the undershoot boundary is determined by a 10g acceleration constraint whereas the overshoot boundary is determined by the minimum entry angle for which a skip to higher altitudes can be prevented. These limiting entry angles define a so-called "entry window," a term often used in expressing entry guidance requirements. A general discussion of these problems of atmospheric entry may be found in reference 1.

The range available to the spacecraft during atmospheric entry is a function of entry angle, vehicle physical and aerodynamic characteristics, vehicle maneuver capability, and constraints placed upon the trajectories. In figure 1 some limiting trajectories are presented. Both long- and short-range trajectories are shown for entry-angle conditions corresponding to the overshoot and undershoot boundaries. Maximum range during entry is extremely sensitive to the altitude constraint placed on the skip trajectory, and the trajectories shown in figure 1 are typical of controlled skips to the fringe of the atmosphere combined with a final glide at a fixed lift-drag ratio. A second performance parameter illustrated in figure 1 is the range-overlap region. This region defines an area of accessible landing points to which the spacecraft can be guided for any entry-angle condition between the overshoot and undershoot boundaries.

The present investigation was undertaken to determine the ability of a pilot to control a spacecraft so as to perform the maneuvers required by the extreme trajectories depicted in figure 1. Satisfactory spacecraft handling qualities will most likely require damping augmentation about all three vehicle axes, and the consequences of automatic damper failures in various combinations were investigated.

A fixed-base simulation employing analog computing equipment and a pilot station with an instrument display and vehicle controls was devised and utilized to conduct the investigation. The instrument display included meter presentations of standard flight data and certain elementary guidance displays. An area of current interest to spacecraft designers is that of minimum display instrumentation required for safe, manned-control entries in which navigational tasks are neglected. Reference 2 presents limited results in which a display of only linear acceleration and the horizon is required. In the present investigation it was desired to determine the effects of entry angle and damper condition on such minimum-display entries.

For long- and short-range entries and entries performed with minimum instrumentation, results are presented of range deviation at the end of entry,

time histories of control inputs, vehicle dynamic and trajectory variables, propellant consumption, and a performance rating indicative of a pilot's ability to perform a given control task. In determining the consequence of automatic damper failure, results of a qualitative nature are obtained by recording pilots' opinions of handling qualities by comparing time histories for damper-in and damper-out conditions and by simply noting whether the pilot could maintain control of the vehicle with the dampers out. As a significant quantitative measure, a comparison was made of the relative magnitudes of errors in final range for a series of entries with dampers in and out. Although the absolute magnitudes of these final errors are not significant, since no realistic guidance system was used, the presence or absence of significant differences in relative errors for the various damper conditions was considered a useful quantitative indication of the ability of a pilot to perform the required maneuvers.

SYMBOLS

A	spacecraft cross-sectional area
a	acceleration resulting from aerodynamic forces
a_n	normal acceleration
$\bar{a}_X$	quickened axial acceleration, $K\left(\frac{1 + \tau_1 s}{1 + \tau_2 s}\right)a_X$
$a_{X,n}$	pilot acceleration task
C_l	rolling-moment coefficient
C_m	pitching-moment coefficient
C_n	yawing-moment coefficient
C_X	longitudinal-force coefficient
C_Y	side-force coefficient
C_Z	normal-force coefficient $\left(C_{Z,o} + C_{Z_\alpha}\alpha\right)$

$$C_{Y_\beta} = \frac{\partial C_Y}{\partial \beta}$$

$$C_{n_\beta} = \frac{\partial C_n}{\partial \beta}$$

$$C_{l_\beta} = \frac{\partial C_l}{\partial \beta}$$

$$C_{Z_\alpha} = \frac{\partial C_Z}{\partial \alpha}$$

$$C_{m_q} = \frac{\partial C_m}{\partial \frac{qd}{2V}}$$

$$C_{n_r} = \frac{\partial C_n}{\partial \frac{rd}{2V}}$$

$$C_{l_p} = \frac{\partial C_l}{\partial \frac{pd}{2V}}$$

d	spacecraft diameter
e_x	downrange error
F	pilot performance factor, $\int \left(a_X - a_{X,n}\right)^2 dt$
g	acceleration due to gravity
h	altitude
I_X	moment of inertia about body X-axis
I_Y	moment of inertia about body Y-axis
I_Z	moment of inertia about body Z-axis
I_{XZ}	product of inertia
K	gain in $\bar{a}_X$ relation
K_p	roll damper gain

K_q pitch damper gain

K_r yaw damper gain

L longitude

$L_p = \frac{\bar{q}Ad^2}{2V} C_{l_p}$

$L_\beta = \bar{q}AdC_{l_\beta}$

$l_i, m_i, n_i (i = 1,2,3)$ direction cosines relating body axes to geographic axes

$M_q = \frac{\bar{q}Ad^2}{2V} C_{m_q}$

$M(\alpha) = \bar{q}AdC_m(\alpha)$

M control moment

m vehicle mass

$N_r = \frac{\bar{q}Ad^2}{2V} C_{n_r}$

$N_\beta = \bar{q}AdC_{n_\beta}$

P period

p,q,r vehicle angular velocity about body X-, Y-, and Z-axis, respectively

$\bar{q} = \frac{\rho V^2}{2}$ dynamic pressure

R range

r_e vehicle distance from center of earth

s Laplace transform variable

t time

$t_{1/2}$ time to damp to one-half amplitude

u,v,w	velocity component along body X-, Y-, and Z-axis, respectively
V	vehicle velocity
W_p	propellant consumption
x	downrange distance in geographic axis system
$\bar{x}$	mean downrange distance
y	crossrange distance in geographic axis system
α	angle of attack
β	angle of sideslip
γ	flight-path angle measured from local horizontal, positive direction up
δ_p	pilot roll-control input, deg/sec^2
δ_q	pilot pitch-control input, deg/sec^2
δ_r	pilot yaw-control input, deg/sec^2
ζ	damping ratio
λ	latitude
ρ	atmospheric density
τ_1,τ_2	time constants in lead filter
ψ,θ,ϕ	Euler angles relating body axes to geographic axes (bank angle ϕ measured in body YZ-plane between horizontal and body Y-axis)
$\bar{\psi}$	flight-path heading angle, measured from initial heading

Subscripts:

X,Y,Z	body axis components
x,y,z	geographic axis components
o	initial condition
R	resultant

max maximum

A dot over a symbol indicates a differentiation with respect to time.

SYSTEM SIMULATION

Spacecraft Description

The spacecraft considered in this investigation is a blunt-face, high-drag capsule and is trimmed to a constant lift-drag ratio of 0.5 as shown in figure 2. The vehicle possesses static longitudinal and directional stability, and maneuverability is obtained by controlling the vehicle roll attitude so as to direct the lift vector in the desired direction. Aerodynamic and mass parameters for the spacecraft are presented in table I. Small throttleable rockets for control of angular motions in three degrees of freedom were assumed in the design. These control rockets had maximum angular acceleration capabilities of 10 deg/sec^2 in roll and 4 deg/sec^2 in pitch and yaw and could be activated by signals from simple rate dampers and/or manual controllers. Lags in the rocket control system were assumed to be negligible.

Computer Programing

A piloted entry simulation requires a six-degree-of-freedom computer program in order to simulate the vehicle dynamic and translational modes. The axis systems selected for defining the vehicle motion are

(1) Rotational degrees of freedom - a body axis system with the X-axis coinciding with the spacecraft axis of symmetry.

(2) Translational degrees of freedom - a moving right-handed set of axes, a geographic axis system, fixed to the spacecraft center of gravity, the Z-axis directed along the local vertical, and the X-axis directed along the horizontal component of the initial velocity vector.

(3) Inertial axes - a coordinate axis system, nonrotating and with its origin at the center of the earth.

Translational motion could be expressed in this particular geographic axis system because the earth was assumed to be spherical and nonrotating and true earth position of the spacecraft was not required. The resulting equations of motion are given in the appendix.

The inclusion of a pilot in the problem necessitated a 1:1 time scale on the analog computing equipment used for the simulation. Problems encountered in the analog programing and methods of solution are discussed in detail in reference 3.

Pilot Station and Display Instrumentation

A sketch of the equipment provided at the pilot station (the instrument panel, pencil-type controller at the right hand, foot pedals, pilot seat, and x-y plotter) is presented as figure 3. The hand controller permits proportional control of motions about the vehicle axis of symmetry (roll) by left and right stick deflections and about the transverse (pitch) axis by fore and aft stick deflections. The foot pedals allow proportional control of yawing motions.

Flight data are displayed on the main instrument panel with time, vehicle velocity, vehicle angular velocities (p,q,r), flight-path heading angle $\bar{\psi}$, and crossrange distance Y displayed on the top row. On the middle row, the first and second meters display normal acceleration a_n and dynamic pressure $\bar{q}$, respectively. In the center is a composite instrument which consists of a three-axis attitude indicator displaying ψ, θ, and ϕ on the ball, with angles of attack α and sideslip β added on two bar indicators in front of the ball. A photograph of the attitude indicator is presented as figure 3(b). The two meters to the right of the attitude indicator display altitude h and altitude rate $\dot{h}$. On the bottom row are presented transverse acceleration a_y, resultant acceleration a_R, quickened axial acceleration $\bar{a}_x$, and range. On the x-y plotter at the pilot's left, vehicle trajectory is plotted. Above the instrument panel is an oscilloscope which presents a composite guidance and situation display.

Spacecraft Dynamics

Although the spacecraft possessed static longitudinal and directional stability, its damping characteristics were poor, and damping augmentation about all three body axes was required. Simple constant-gain rate dampers were simulated, and the vehicle dynamic characteristics for both a low and a maximum dynamic-pressure condition are presented in table II. The damper gains were selected, not from any handling-qualities criteria, but from high-dynamic-pressure simulated entries in which rapid maneuvers were required. The gains chosen were values which produced vehicle dynamics acceptable to the pilots over the range of flight conditions considered. In particular, the roll rate gain was a compromise between desired roll damping and roll-control effectiveness. During the investigation simulated entries were made for many damper combinations; however, results are presented herein for only the three conditions of all dampers in, pitch damper only, and all dampers out.

DISPLAY DEVELOPMENT AND PILOTING TASKS AND PROCEDURES

Long-Range Entries

Choice of display parameters.- The accomplishment of long-range entries by means of skips to high altitudes requires a special guidance technique. In

this investigation an arbitrary altitude limit of 400,000 feet was imposed on the skip trajectories. With this altitude limit, the skip trajectories were constrained to very moderate skip-outs, in which aerodynamic trajectory control was ineffective for only a short time. No consideration was given to very high and long skip-outs, which require very precise control of exit conditions. (See, for example, ref. 4.)

In order for a skip to high altitude to be accomplished by manual control, the pilot must control precisely the vehicle exit flight conditions through control of vehicle lift and drag. A method which has been used in the past in simulator studies (ref. 5) to accomplish high altitude skips was to program a reference trajectory of altitude as a function of altitude rate in an oscilloscope display.

The reference-trajectory method of reference 5 was adopted for this investigation except that altitude was replaced by axial acceleration as a primary trajectory variable. Axial acceleration was selected as a more practical variable for a flight system for the following reasons:

(1) Axial acceleration is simply, accurately, and reliably measured onboard an entry vehicle.

(2) Acceleration is sensitive to the actual atmospheric environment and avoids the errors encountered from using a model atmosphere.

Altitude rate, the other parameter used in controlling to the reference trajectory, would probably be obtained from an onboard inertial measurement unit. The accuracy of altitude-rate determination, as discussed in reference 6, appears to be adequate for this application.

Reference-trajectory determination.- A simple control technique which produces a skipping, long-range trajectory for the steep (high g) entry path was investigated in the initial phase of the simulator program. Piloted entries were made, with the vehicle roll-control system and dynamic characteristics simulated, to determine controllability boundary curves for skipping to a 400,000-foot altitude. For these runs a zero-bank-angle ($\phi = 0^\circ$) entry was made through pull-out and into a climb, to establish a skipping trajectory. At some point after pull-out, a 180° roll to inverted flight, using full roll-control capability, was made to avoid skipping above the altitude limit. This technique gets the vehicle out of the high-energy-loss (high-g) condition very quickly. The boundary curve for an initial entry angle of $-7\frac{1}{2}^\circ$ is shown in figure 4 in terms of the two variables, axial acceleration and altitude rate. Only positive altitude rates are shown, since control of skip-up is initiated following pull-out. In observing the skipping constraint of the investigation the pilot must, in general, control the spacecraft to remain inside (to the left of) the boundary.

Although this boundary curve represents a trajectory with a maximum altitude too sensitive to the time of the 180° roll maneuver to be used as a realistic piloting task, it was valuable as a limiting curve for the practical

maneuver. With the boundary curve as a guide, the next step was to generate a reasonable piloting task which would not have such critical characteristics but would result in a skipping trajectory of long-range potential. The reference curve which was chosen is shown as the dashed curve in figure 4 and is a fairly conservative approximation to the limiting curve. This reference curve produces a skip to 360,000 feet and a final range capability of 4,300 nautical miles.

Display mechanization.- To facilitate the pilot control of the spacecraft to the reference-trajectory conditions, an oscilloscope was used. On it the reference conditions a_x and $\dot{h}$ were continuously displayed along with the corresponding vehicle conditions by a moving pip as shown in figure 5. Inasmuch as the presentation is restricted to positive altitude rates, the $\dot{h} = 0$ axis is the locus for zero and all negative values of altitude rate. In addition to the trajectory conditions, spacecraft bank angle was presented on the scope to reduce pilot scanning. Bank angle was indicated by a generated straight line which rotated about the scope center to indicate the direction of the vehicle lift (fig. 5). For example, a vertical orientation, with the indicator directed toward the top of the scope, denotes an unbanked attitude ($\phi = 0^\circ$) with the vehicle lift acting upward. Details of the scope mechanizations have been discussed in reference 3.

Piloting procedure.- The tasks required of the pilot in following the reference curve for long range are:

(1) Maintain zero bank angle through the initial entry to just past pull-out (minimum altitude, maximum deceleration). At the start of the simulated entry the pip denoting vehicle conditions would be at the lower left-hand corner, indicating zero aerodynamic acceleration and negative altitude rate. As the vehicle enters the atmosphere and acceleration builds up, the pip moves up the $\dot{h} = 0$ axis to a peak acceleration at pull-out. Following pull-out, the pip moves rapidly away from the $\dot{h} = 0$ axis as climb rate builds up.

(2) Establish a constant climb rate of 1200 feet per second by rolling the vehicle to a bank angle of approximately 90°. The spacecraft at this time is approximately at circular orbital velocity and hence at a radial acceleration of nearly zero, so that the lift must be directed to either side to maintain a constant vertical velocity (altitude rate). As the altitude increases at this constant rate, the aerodynamic acceleration will decrease, with the pip moving down the line $\dot{h} = 1200$.

(3) Reduce climb rate in proportion to the reduction of aerodynamic deceleration during climb, as specified by the straight-line skip-out boundary. The trajectory control available to the pilot is proportional to the aerodynamic acceleration and, to avoid skipping to excessive altitudes, climb rate must be reduced before maneuvering control (vehicle lift) is lost. To decrease climb rate according to the reference curve, the pilot must maintain a bank angle of approximately 160°.

(4) Establish and hold a final climb rate of 600 feet per second. As the acceleration reduces to zero, a varying bank angle of 90° to 0° was required to

maintain climb rate. In this simulation, atmospheric density was reduced to zero for altitudes above 300,000 feet and, consequently, trajectory control capability terminated at this altitude. From this point the spacecraft was in a ballistic trajectory and skipped to an altitude of about 360,000 feet. The choice of 600 feet per second for the final climb rate was somewhat arbitrary. Variation of this final climb rate is, of course, an effective method of varying the final range in long-range entries.

In addition to the downrange task, the pilot had a crossrange task which was to terminate the entry with zero crossrange distance. For this vehicle with a fixed lift-drag ratio, the piloting tasks are difficult because bank angle is the only parameter available to the pilot for controlling both downrange and crossrange distances. For example, the downrange maneuver of climbing at 1200 feet per second may be performed by holding the bank angle near 90°. However, this would cause such large lateral-heading and crossrange deviations to develop in the skip that the crossrange distance could not be finally reduced to zero. Therefore, bank angles of both 90° and 270° must be used in the skip. Figure 6(a) shows a_x plotted against $\dot{h}$ for a maneuver which tries to follow the prescribed task closely by performing a series of rapid roll maneuvers and employing a bank angle of 270° as well as 90°. This maneuver is only practical with all dampers operating. The maneuver shown in figure 6(b) consisted simply of a gradual roll from 90° to 270° bank angle, with the reference curve used as a guide. With practice, the gradual maneuver was found satisfactory for consistent trajectory control even with all dampers out. Note that the undamped-vehicle oscillations evident in this case did not become excessive.

Range control during the final glide is observed by flying to a reference trajectory plotted on an x-y plotter presentation of altitude as a function of downrange distance. The reference trajectory covers the altitude range of 200,000 feet to 100,000 feet and can be seen in figure 7. This figure shows complete dampers-in and dampers-out trajectories and also shows how the short terminal reference trajectory is used for terminal guidance.

Short-Range-Entry Display

The technique used by the pilots in performing short-range entries was to pull down (fly at 180° bank angle) until a designated axial-acceleration a_x level was reached and then to maintain this a_x level for the remainder of the entry. This task can be more easily accomplished if the pilot also monitors altitude rate which acts as a lead signal. Since both the axial acceleration and the altitude rate were already mechanized on the oscilloscope, it was adapted to this type of entry by presenting negative values of altitude rate in place of positive values used for long-range entries. Preliminary simulation runs of this type indicated that the display of quickened acceleration (acceleration signal passed through a lead filter which introduces some acceleration rate into the signal) made the acceleration control task much easier. Hence, the basic display evolved for these entries was a composite presentation of quickened axial acceleration, altitude rate, and bank angle.

In selecting the acceleration level to be used as the task, simulation runs were made at both 6g and 8g. The range difference for these two conditions was only about 150 miles and did not appear significant when weighed against the increased discomfort and danger for the crew in an 8g entry. Hence, an acceleration level of 6g was selected for the piloting task.

RESULTS AND DISCUSSION

Long-Range Entries

In long-range entries with steep-entry condition $\left(\gamma_o = -7\frac{1}{2}^\circ\right)$ the pilot tasks were to achieve a downrange distance of 4300 nautical miles and a crossrange distance of 0 miles at a terminal altitude of 100,000 feet. In accomplishing these tasks the pilot navigated by crossrange and heading-angle meters, the nominal program of acceleration as a function of altitude rate presented on the scope, and an x-y plotter presentation of generated trajectory (altitude plotted against downrange distance) along with the terminal reference trajectory.

Results are presented in figures 7 to 9 for two long-range entries, one being made with all dampers in and the other with all dampers out. The piloting procedure used for controlling crossrange distance differed in the two runs, as shown in figure 6; for the task shown in this figure, the pilot used the rapid rolling technique for all dampers in and the slow rolling technique for all dampers out. The trajectories for these two damper conditions, as recorded on the x-y plotter, are presented in figure 7. With dampers either in or out the pilot did a good job of completing the range tasks. No critical degradation of ability to control the trajectory is evident with the automatic-damping equipment inoperative, as long as the pilot used the slow rolling technique.

Time histories of pertinent motion and control variables are presented in figure 8 for all dampers in. With all modes well damped, no stability problems existed and the pilot devoted his attention to the rolling maneuvers required by the tasks. Results are presented only for the initial entry and up to the peak of the skipping trajectory to illustrate the ease with which the vehicle is controlled. Note the simplicity of the pilot's roll-control inputs and the ability to use full, rapid inputs.

With all dampers out (fig. 9), no particular problems existed during the initial penetration of the atmosphere (up to 200 seconds); the primary roll maneuver required was a slow roll through 270°. Note, however, that the pilot never used full control, but carefully applied a sequence of small inputs to obtain the required motion without excessively disturbing the vehicle. Upon exiting the atmosphere ($t > 200$), the pilot only applied control periodically, to prevent excessive divergence of α and β from their trim values and to keep near zero bank angle, as shown in figures 9(a) and 9(b). It is seen in figure 9(b) that the pilot had no difficulty returning to the trim conditions

when the second entry occurred and the static stability became effective. From here on, the pilot controlled the bank angle as necessary to complete the downrange and crossrange tasks. Occasional pitch and yaw control pulses were continually required to damp transient motions.

The final range errors and total propellant consumption are presented in figure 10 for all the complete long-range entries performed. The conclusion is that the pilot did as good a job of accomplishing the primary (range) tasks with all dampers out as with all dampers in and with a considerable reduction in propellant used. The range results for all dampers out indicate one run (denoted run 2) with a significantly larger downrange error than the other runs. In this particular simulated entry the pilot permitted crossrange distance to build up during the initial entry and skip-up. During the final glide, in an attempt to reduce crossrange distance to zero, the pilot made a number of bank maneuvers which had the effect of reducing downrange capability. As a result the pilot failed to achieve the required downrange distance by the indicated range error. With all dampers out the pilot rated the vehicle "acceptable for emergency use only" because of the attention required to monitor and damp the vehicle characteristic modes.

With all dampers in, several factors contribute to the increased propellant consumption. First, it should be emphasized that only one set of control rockets was assumed for each vehicle axis, and that pilot-control and rate damper signals were combined to form one net thrust signal. Hence, in rolling maneuvers, the roll rate damper modifies the pilot input to give smoother and more precise maneuvers. This leads to a tendency for less fuel usage, since there is less likelihood of extra thrust reversals in residual oscillations. In practice, however, the pilot inputs were larger with dampers in and the pilots performed the rolling maneuvers more rapidly, since this configuration (being "well damped") was easier to control. Since the fuel used in a bank maneuver is directly proportional to the roll rate used, this leads to a tendency to use more fuel with dampers operating. Analysis of the fuel consumption results indicates, however, that these two effects tend to cancel each other, since the increased fuel consumption with dampers operating seems to arise primarily from yaw-damper operation. The probable reason for this effect can be shown by a simple analysis.

Consider the side-force equation, in body axes:

$$V(\dot{\beta} + r \cos \alpha - p \sin \alpha) = a_Y$$

Since the roll jets operate about the body axes, each rolling maneuver tends to create some steady value of p, the rolling velocity. Within the atmosphere, the directional stability effectively coordinates the turn, keeping the sideslip angle β small, so that the desired coordination condition on yawing $r = p \tan \alpha$ is approximately maintained. Therefore, it is clear that the yaw damper will waste fuel in each attempted roll maneuver, by working against this desired yawing velocity. Two possible ways to eliminate this condition might be to use stability axis yaw rate as the yaw damper input or to use a

washout circuit on the yaw damper signal so that it would not oppose steady yaw rates.

It should be emphasized that the errors shown in figure 10 are not to be considered representative of the absolute accuracy which could be obtained with an actual guidance system. Range displays of finer resolution would undoubtedly have reduced range errors, but the crude terminal guidance used was adequate for the purposes of this investigation.

Short-Range Entries

The minimum range limit of the landing footprint is fixed by the shortest range which can be achieved from entries on the overshoot boundary of the entry corridor. Short-range entries are also of interest in emergencies, when it may be necessary to get down as quickly as possible. A number of piloted runs were made in this condition to assess the effect of damper configuration and display configuration.

Effect of automatic dampers.- Results of entries in which the pilot task was to hold 6g and terminate with zero crossrange distance are shown in figures 11 to 13. For these runs the pilot utilized the composite display of quickened axial acceleration, altitude rate, and bank angle described previously in the discussion of display development. Dynamic variables, trajectory parameters, and roll-control data are presented in figure 11 for two damper conditions - all dampers in and all dampers out. Frequent roll-control inputs were required in order to control simultaneously the deceleration and the off-course range. With all dampers out, the pilots used smaller and less abrupt control motions in order to avoid violent transient motions in pitch and yaw. Note in figure 11(a) the low level to which oscillations in α, β, and a_R were held. The axial acceleration plotted in figure 12 shows that without dampers there is a considerable reduction in the precision of controlling acceleration.

In figure 13 results of downrange and crossrange distances, fuel consumption, and performance factor are shown for a number of entries with dampers in and out. Performance factor scores the pilot on his success in accomplishing the acceleration task during an entire run and is defined as $\int \left(a_X - a_{X,n}\right)^2 dt$. The average downrange distance for these entries was 1035 miles with dampers in and 1060 miles with dampers out. More variation appeared in the results for dampers out than for dampers in. Much less fuel was used without dampers (21 pounds compared with 58 pounds), whereas pilot task performance was worse as was borne out by the acceleration records.

With dampers out, the vehicle was rated "acceptable for emergency use only" because of transient oscillations induced by the required rolling maneuvers and the high level of pilot attention required to accomplish the task. This is illustrated in figure 13 for one entry in which an off-course range of 33 miles

resulted because the pilot overlooked his heading task in the presence of the acceleration task.

Entries with trajectory parameters displayed on individual meters.- Several entries were made with all dampers out to determine the effect of increased pilot scanning time required when individual meter displays of quickened acceleration, altitude rate, and bank angle were used. Reference to figure 3 will indicate the scanning required to observe these variables.

Results of these entries are presented in figure 14 in bar-graph form and are compared with entries in which the composite scope display was used. There is little difference to be noted in downrange and crossrange distances and propellant consumption; however, the performance-factor results indicate that the pilot did a poorer job of controlling the vehicle to 6g when using individual meter presentations. For example, the entry for which the performance factor was 137 was one in which the axial acceleration varied between a maximum of 12g and a minimum of 2g. These entries were difficult because of the effort required in accomplishing the task, and the pilots definitely preferred the composite scope display.

Minimum-Display Entries

Much attention is being given to systems for guiding returning space vehicles to specific destinations. A diverse problem encountered when considering backup systems and simplicity is the determination of minimum control and display systems with which the pilot can safely traverse the atmosphere with only remote interest in range. With this problem in mind and from the experience obtained with long- and short-range entries, it was speculated that a pilot could make a safe entry given only a knowledge of vehicle acceleration and bank angle. For a blunt-faced capsule such as that considered herein the deceleration is almost entirely along the axis of symmetry. Therefore, axial acceleration was selected for display.

Trajectory plots of h against X are presented in figure 15 for a condition of three-axis damping in which only axial acceleration and bank angle were displayed to the pilot. The upper curve is for a shallow entry and the lower curve, a steep entry. For both entries the pilot task was to establish and hold a 2g deceleration. This value was selected as a minimum acceleration which would produce safe and tolerable entries for any conditions within the entry corridor. For shallow entries skip trajectories must be avoided for supercircular velocities, and figure 15 shows that a 2g deceleration $\left(\text{for } \gamma_o = -5\frac{1}{2}^\circ\right)$ is sufficient to accomplish this. In the shallow entry the pilot enters at a roll attitude of 180° until the 2g condition is reached. For the remainder of the entry, deceleration is controlled through bank angle. Because the trajectory characteristics consist of a long-period, lightly damped oscillation, the task cannot be accomplished with precision. Deceleration varied between 2g and 3g on the shallow entry.

In the steep entry the pilot enters in an unbanked ($\phi = 0^\circ$) attitude and, by definition, a 10g condition exists at pull-out. After pull-out bank angle is controlled in order to get on a 2g trajectory. As a result of the higher g environment at pull-out the downrange distance is less in the steep entry. At both steep- and shallow-entry conditions the pilot did a good job of controlling the trajectory with only bank angle and deceleration displayed.

Some entries were made in vehicle conditions simulating automatic damper failures, and results are presented for pitch damping only and for all dampers out with an initial entry angle of $-5\frac{1}{2}^\circ$. For only the pitch-damper-in condition, the results include sample time histories of pertinent variables presented in figure 16, sample trajectory data in figure 17, and range and fuel-consumption data for a series of runs in figure 18. For this damper condition the vehicle longitudinal dynamics presented no problem, and the pilot devoted his attention to controlling bank angle. The task of simultaneously keeping sideslip small was relatively easy. Angle of attack was not recorded in this series, but the pitching-velocity transients were also small in magnitude. The acceleration time history is oscillatory as expected, and this variation shows up in the trajectory plot also. The results for six runs indicated an average downrange distance of 1845 miles with an rms (root mean square) deviation of 56 miles, an rms crossrange deviation of 30 miles, and an average fuel consumption of 26 pounds.

Results for runs with all dampers out are presented as time histories of pertinent variables in figure 19, sample trajectory data in figure 17, and range and fuel-consumption data in figure 18. Time histories of the dynamic variables (fig. 19(a)) indicate that the control task was more difficult because of the neutrally stable condition of both longitudinal and lateral modes. Entries in this damper condition were accomplished only when an added display of vehicle angular velocities was provided. With these data displayed the pilot damped transient motions at various times during the entry, as is evidenced in the time histories for angle of attack and sideslip. Considerable deviation of acceleration from the desired 2g value is noted, and an oscillatory trajectory resulted. For seven runs (fig. 18) the downrange distance averaged 1750 miles with an rms deviation of 90 miles, the rms crossrange deviation was 40 miles, and the fuel consumption averaged 25 pounds.

Significant results are that controlled safe entries could be made with pitch damping augmentation only, with a knowledge of bank attitude and acceleration. However, given the angular-rate information in addition to bank attitude and acceleration, the pilot was consistently able to carry out the task of simultaneously keeping the oscillations damped and performing a safe entry, even with no damping augmentation.

CONCLUDING REMARKS

A piloted analog simulation study of a blunt-faced capsule entering the earth's atmosphere at parabolic velocity was made. The problems investigated

were the ability of the pilot to control the vehicle for long- or short-range trajectories and the displays necessary to aid the pilot in this task.

With the aid of an integrated guidance and situation display and a terminal-reference-trajectory display, the pilots were able to accomplish the maneuvers required to obtain long-range trajectories with or without three-axis damping augmentation. However, without damping augmentation the vehicle was rated by the pilot as "acceptable for emergency use only" because of the attention required in controlling vehicle attitude.

In performing short-range entries, a constant-acceleration task was given the pilot. With a display of quickened acceleration, successful entries were performed with or without damping augmentation. However, for entries without dampers, pilot task performance was lower and total range variation for a number of entries was greater.

Entries were performed to determine the minimum display instrumentation required for a safe entry. With a display of only bank angle and axial acceleration, safe entries could be performed with only pitch damping augmentation by maintaining a 2g acceleration condition. With no damping augmentation, it was necessary to add a display of angular velocities; the pilot could then make safe entries by periodically damping the vehicle motions through the use of reaction controls.

Langley Research Center,
National Aeronautics and Space Administration,
Langley Station, Hampton, Va., December 2, 1964.

APPENDIX

EQUATIONS OF MOTION

Equations defining the angular and translatory motions of the spacecraft are given herein. Moment equations are written in a body axis system and translation equations are written in a geographic axis system in which the X-axis coincides with the horizontal component of the initial velocity vector. Assumptions pertinent to the equations are

(1) Axis system fixed to center of earth defines an inertial set

(2) Earth is spherical and nonrotating

(3) Acceleration due to gravity is considered constant

(4) Out-of-plane velocity V_y and displacement angle λ are small so that $\tan \lambda \approx \lambda$

When assumption (4) is introduced and higher order terms are neglected, the following translational equations result:

Translation equations in geographic axis system:

$$\dot{V}_x = l_1 a_X + m_1 a_Y + n_1 a_Z + \frac{V_x V_z}{r_e}$$

$$\dot{V}_y = l_2 a_X + m_2 a_Y + n_2 a_Z - \frac{V_x^2 \lambda}{r_e}$$

$$\dot{V}_z = l_3 a_X + m_3 a_Y + n_3 a_Z + g - \frac{V_x^2}{r_e}$$

Moment equations in body axis system:

$$I_X \dot{p} - \left(I_Y - I_Z\right) qr - I_{XZ} \dot{r} - I_{XZ} pq = L_p p + L_\beta \beta + M_x$$

$$I_Y \dot{q} - \left(I_Z - I_X\right) pr - I_{XZ} r^2 + I_{XZ} p^2 = M_q q + M(\alpha) + M_y$$

$$I_Z \dot{r} - \left(I_X - I_Y\right) pq - I_{XZ} \dot{p} + I_{XZ} qr = N_r r + N_\beta \beta + M_z$$

APPENDIX

Euler angle rate equations:

$$\dot{\phi} = p + q \sin \phi \tan \theta + r \cos \phi \tan \theta$$

$$\dot{\theta} = q \cos \phi - r \sin \phi + \dot{L} \cos \psi$$

$$\dot{\psi} = r \frac{\cos \phi}{\cos \theta} + q \frac{\sin \phi}{\cos \theta}$$

Direction cosines:

$$l_1 = \cos \psi \cos \theta$$

$$l_2 = \sin \psi \cos \theta$$

$$l_3 = -\sin \theta$$

$$m_1 = \cos \psi \sin \theta \sin \phi - \sin \psi \cos \phi$$

$$m_2 = \sin \psi \sin \theta \sin \phi + \cos \psi \cos \phi$$

$$m_3 = \cos \theta \sin \phi$$

$$n_1 = \cos \psi \sin \theta \cos \phi + \sin \psi \sin \phi$$

$$n_2 = \sin \psi \sin \theta \cos \phi - \cos \psi \sin \phi$$

$$n_3 = \cos \theta \cos \phi$$

Aerodynamic accelerations in body axis system:

$$a_X = \frac{\bar{q}A}{m} C_X$$

$$a_Y = \frac{\bar{q}A}{m} C_{Y_\beta} \beta$$

$$a_Z = \frac{\bar{q}A}{m} C_Z$$

Aerodynamic relations:

$$\begin{bmatrix} u \\ v \\ w \end{bmatrix} = \begin{bmatrix} l_1 & l_2 & l_3 \\ m_1 & m_2 & m_3 \\ n_1 & n_2 & n_3 \end{bmatrix} \begin{bmatrix} V_x \\ V_y \\ V_z \end{bmatrix}$$

$$\bar{q} = \frac{1}{2}\rho V^2$$

$$\tan \alpha = \frac{w}{u}$$

$$\left.\begin{aligned} \gamma &= -\frac{V_z}{V} \\ \beta &= \frac{v}{V} \\ \bar{\psi} &= \frac{V_y}{V_x} \end{aligned}\right\} \text{Result of small-angle assumptions}$$

Position data:

$$\dot{L} = \frac{V_x}{r_e}$$

$$\dot{\lambda} = \frac{V_y}{r_e}$$

$$\dot{h} = -V_z$$

Vehicle control system:

Control-moment inputs are the sum of pilot-applied moments and automatic damper inputs. These equations are

$$\frac{M_X}{I_X} = \delta_p - K_p p$$

$$\frac{M_Y}{I_Y} = \delta_q - K_q q$$

$$\frac{M_Z}{I_Z} = \delta_r - K_r r$$

where K_p, K_q, K_r are constant damper gains and δ_p, δ_q, δ_r are pilot inputs. Limits are placed on M_X/I_X, M_Y/I_Y, M_Z/I_Z, δ_p, δ_q, δ_r.

REFERENCES

1. Chapman, Dean R.: An Analysis of the Corridor and Guidance Requirements for Supercircular Entry Into Planetary Atmospheres. NASA TR R-55, 1960.

2. Young, John W.; and Barker, Lawrence E., Jr.: Moving-Cockpit-Simulator Study of Piloted Entries Into the Earth's Atmosphere for a Capsule-Type Vehicle at Parabolic Velocity. NASA TN D-1797, 1963.

3. Moul, M. T.; White, E. J.; and Schy, A. A.: Analog Simulation of Piloted Earth Reentry at Parabolic Velocity. NASA paper presented at Intern. Symp. Analogue and Digital Tech. Appl. to Aeron. (Liege, Belgium), Sept. 9-12, 1963.

4. Young, John W.: Study of the Use of Terminal Control Techniques for Guidance During Direct and Skip Entries for a Capsule-Type Vehicle at Parabolic Velocity. NASA TN D-2055, 1964.

5. Young, John W.; and Russell, Walter R.: Fixed-Base-Simulator Study of Piloted Entries Into the Earth's Atmosphere for a Capsule-Type Vehicle at Parabolic Velocity. NASA TN D-1479, 1962.

6. White, John S.: Investigation of the Errors of an Inertial Guidance System During Satellite Re-Entry. NASA TN D-322, 1960.

TABLE I.- SPACECRAFT PHYSICAL AND AERODYNAMIC CHARACTERISTICS

A, sq ft	140
d, ft	13.3
I_X, slug-ft^2	3980
I_Y, slug-ft^2	3720
I_Z, slug-ft^2	3160
I_{XZ}, slug-ft^2	-286
m, slugs	268
C_{Y_β}, per rad	-0.22
C_{n_β}, per rad	0.103
C_{l_β}, per rad	0.011
C_{Z_α}, per rad	-0.29
$C_{Z,o}$	-0.05
C_{l_p}, per rad	-0.1
C_{m_q}, per rad	-0.2
C_{n_r}, per rad	-0.2
K_p	0.2
K_q	1.6
K_r	1.6
$\delta_{p_{max}}$, deg/sec^2	10
$\delta_{q_{max}}$, deg/sec^2	4
$\delta_{r_{max}}$, deg/sec^2	4
τ_1, sec	10
τ_2, sec	1

C_m and C_X were nonlinear functions of α (fig. 2)

TABLE II.- SPACECRAFT DYNAMIC CHARACTERISTICS

(a) Longitudinal short-period mode

$\bar{q}$	With damper			Without damper		
	P	$t_{1/2}$	ζ	P	$t_{1/2}$	ζ
50	4	0.9	0.5	4	∞	0
750	1	.9	.1	1	∞	0

(b) Lateral modes

$\bar{q}$	With dampers					Without dampers				
	Dutch roll mode				Roll mode	Dutch roll mode				Roll mode
	P	$t_{1/2}$	ζ	ϕ/β	$t_{1/2}$	P	$t_{1/2}$	ζ	ϕ/β	$t_{1/2}$
50	4	0.9	0.5	0.1	2.5	4	∞	0	0.1	∞
750	1	.9	.1	.1	2.6	1	∞	0	.1	∞

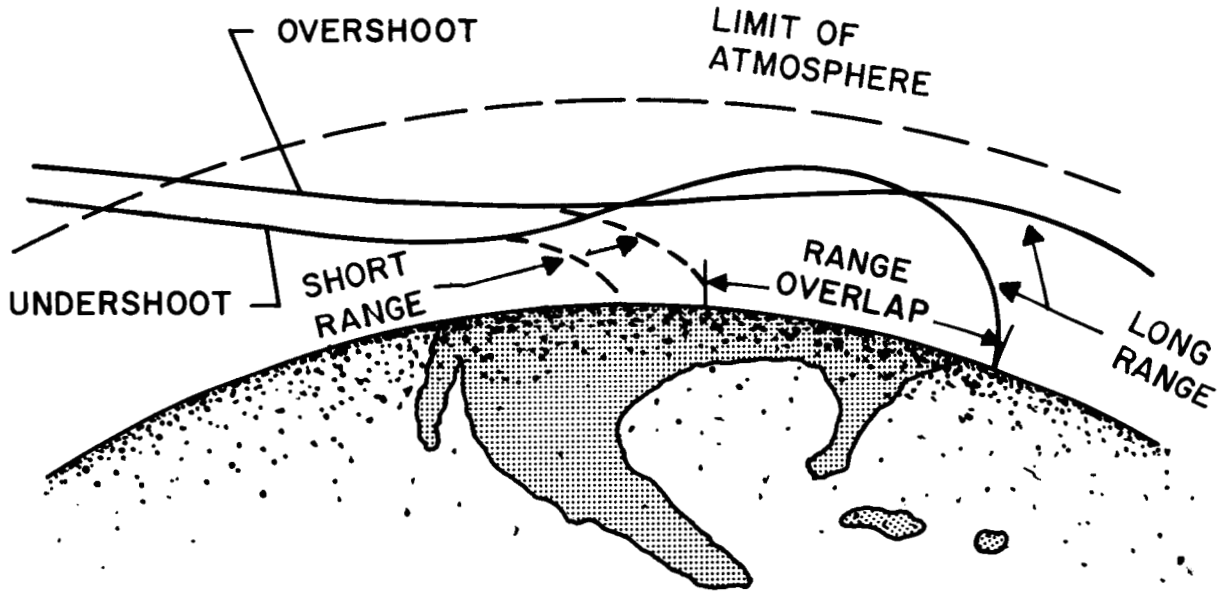

Figure 1.- Long- and short-range entries at parabolic velocity.

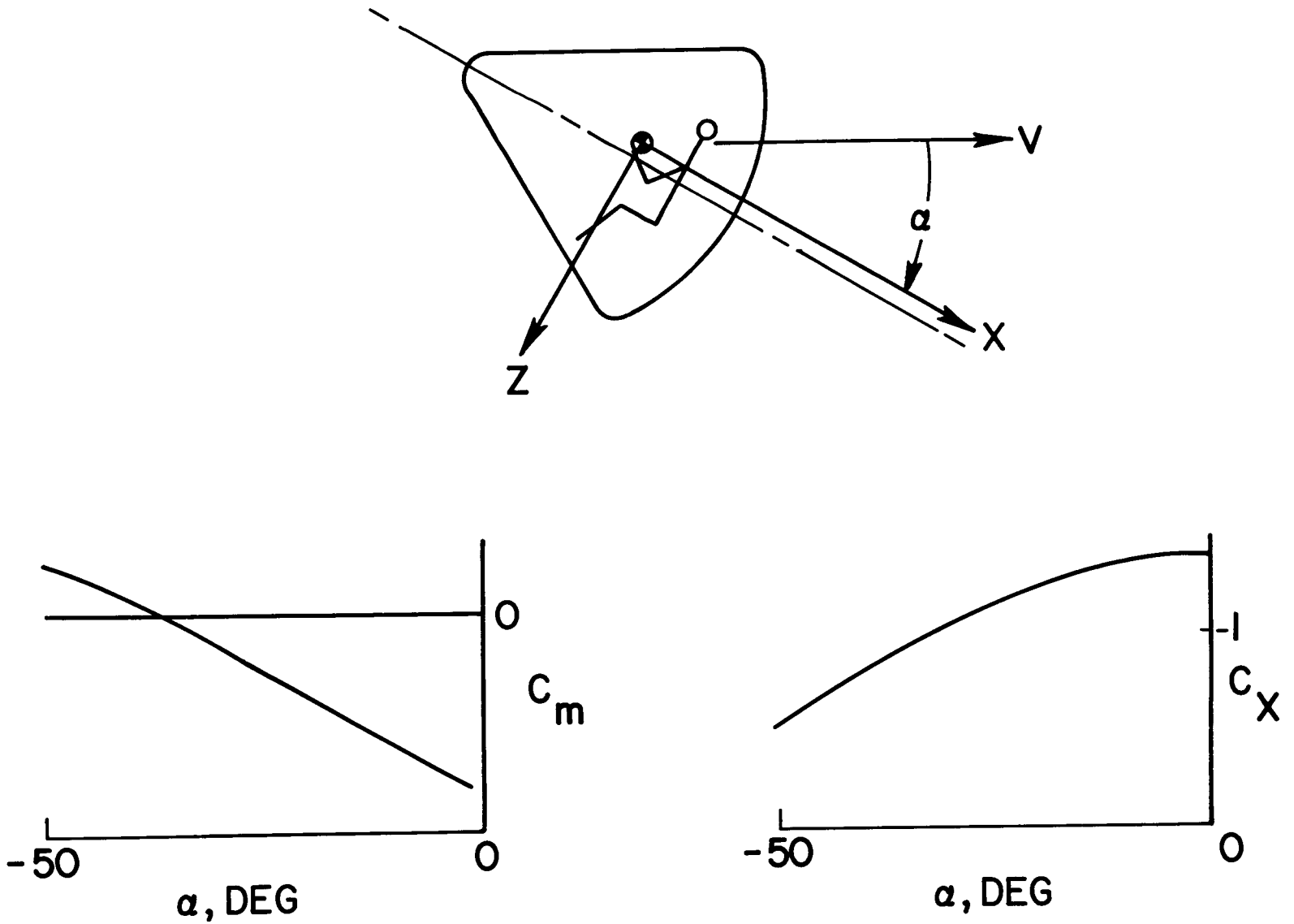

Figure 2.- Vehicle configuration and aerodynamic characteristics.

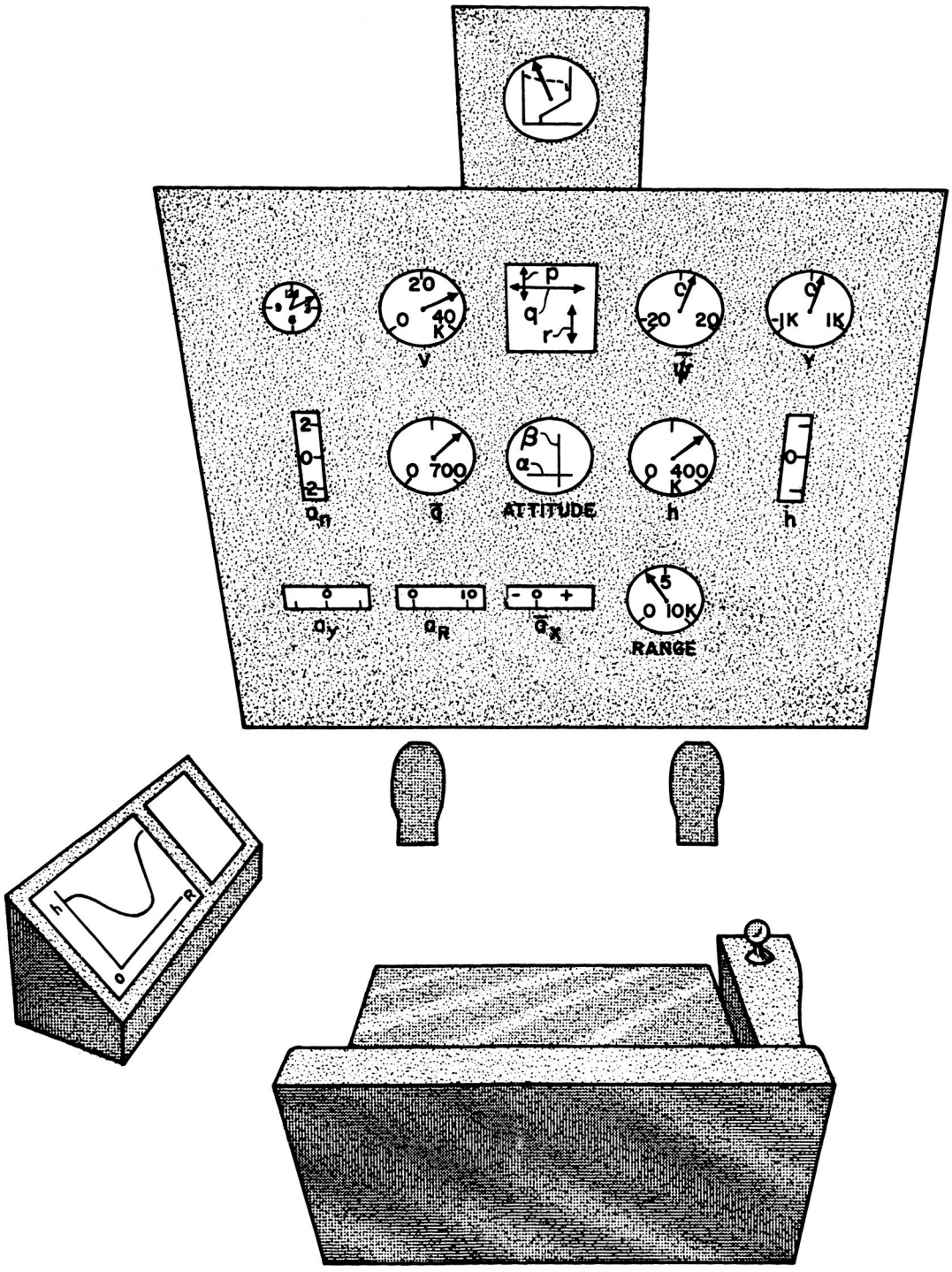

(a) Pilot station and instrument display.

Figure 3.- Simulator equipment.

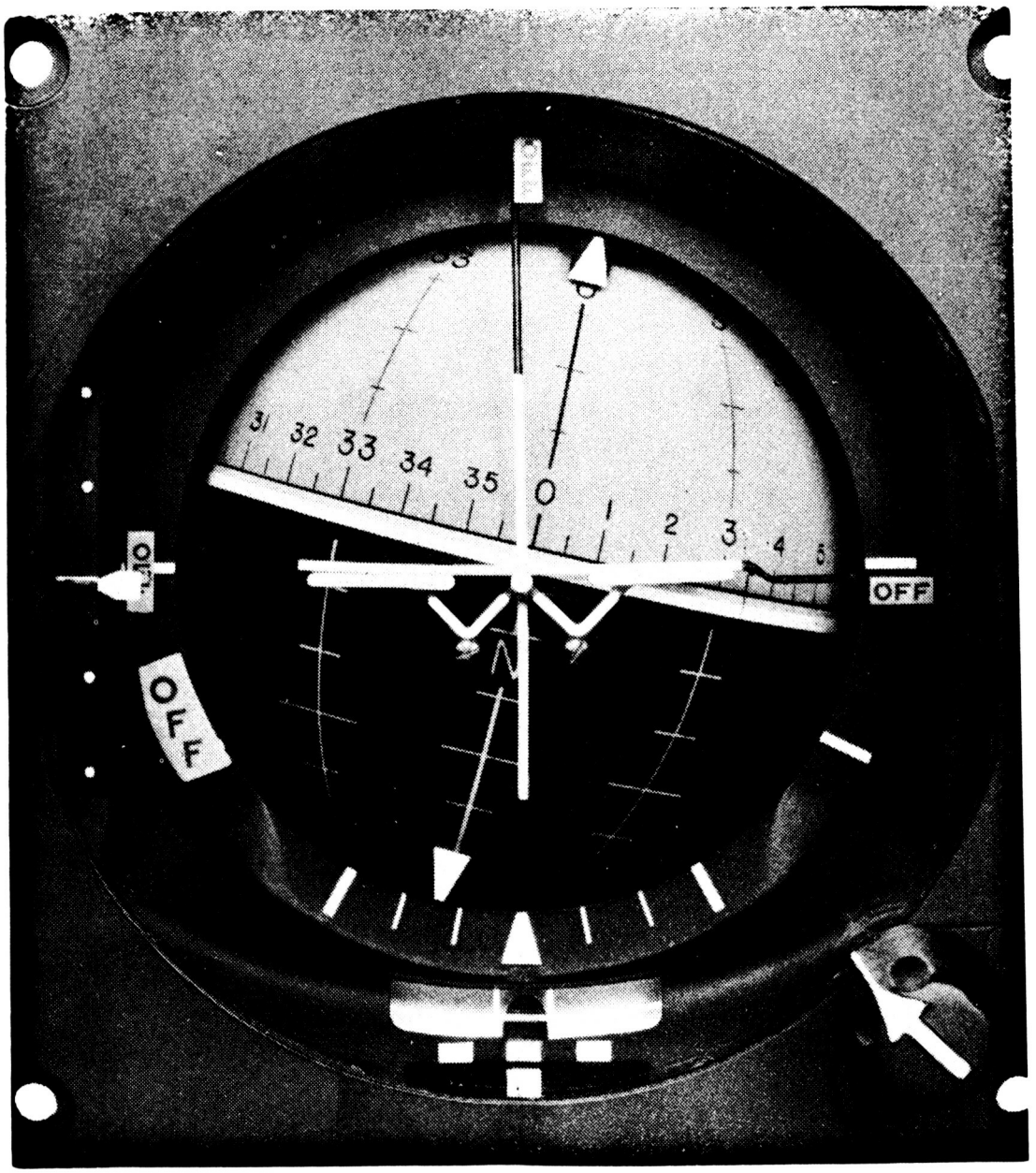

(b) Three-axis attitude indicator. L-64-10219

Figure 3.- Concluded.

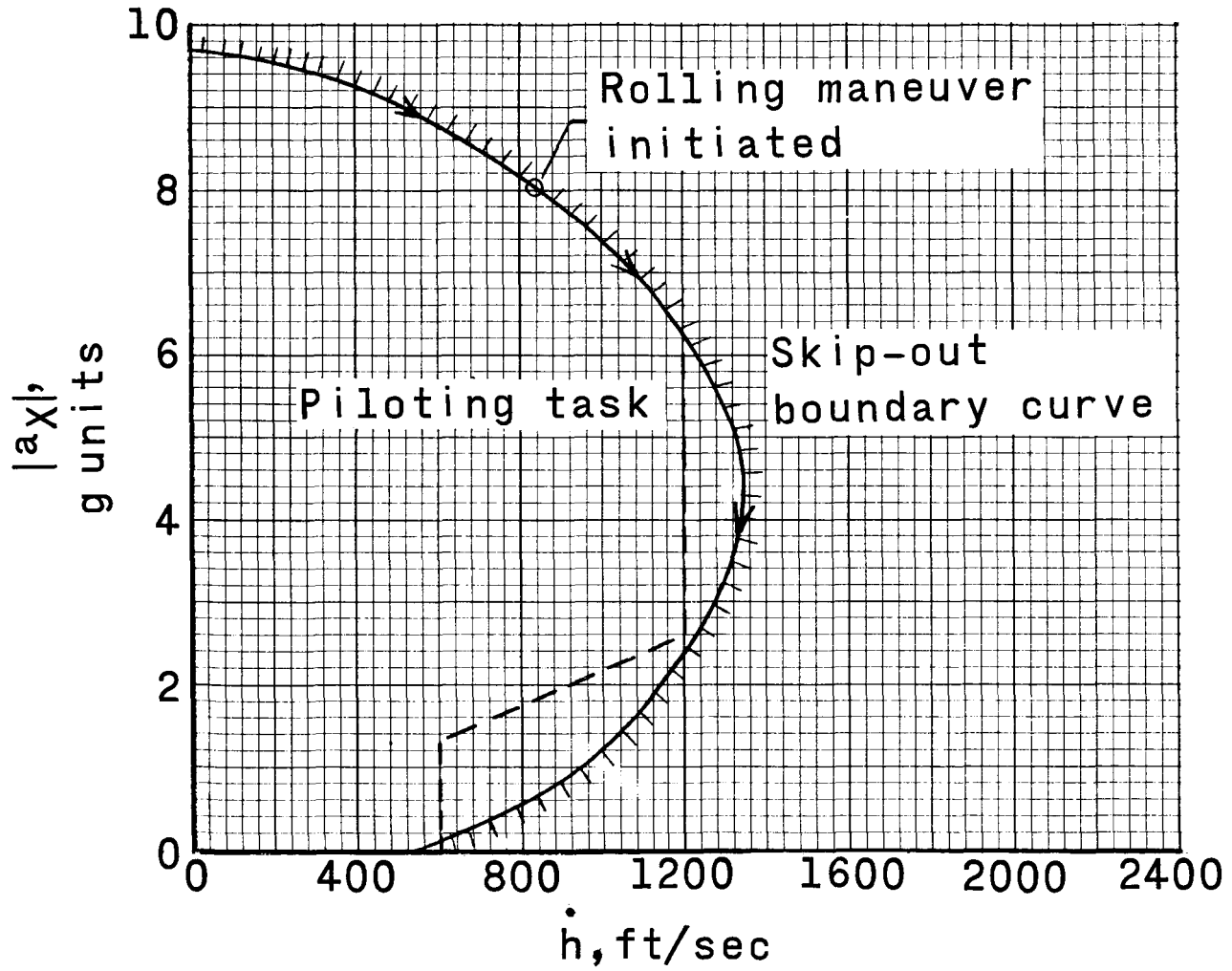

Figure 4.- Piloting task for control of skip. In steep entry, $\gamma_o = -7\frac{1}{2}^\circ$.

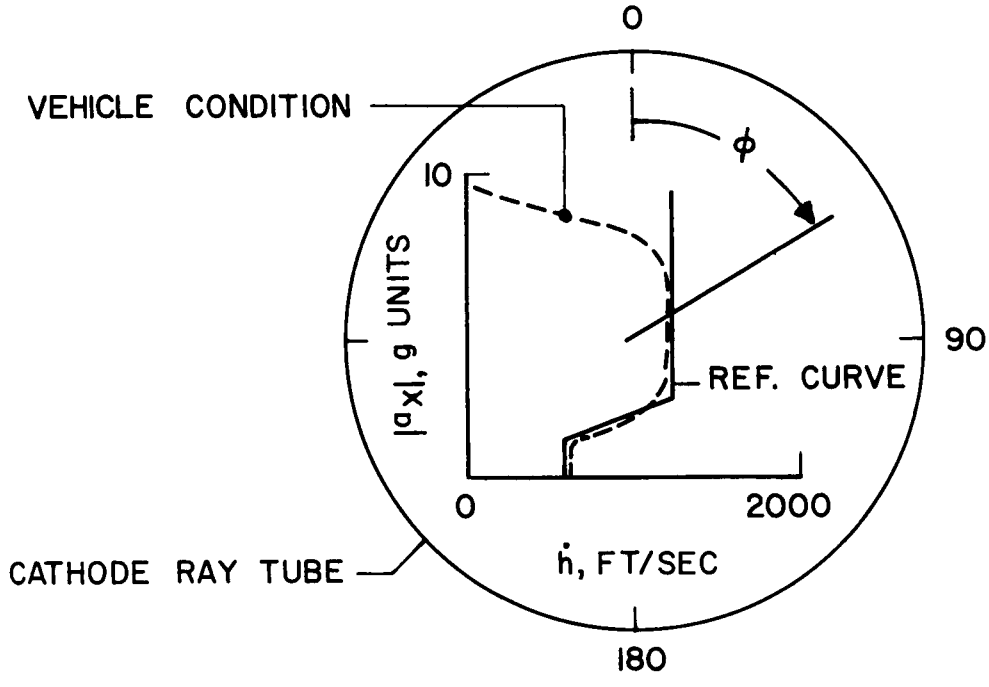

Figure 5.- Trajectory guidance and situation display.

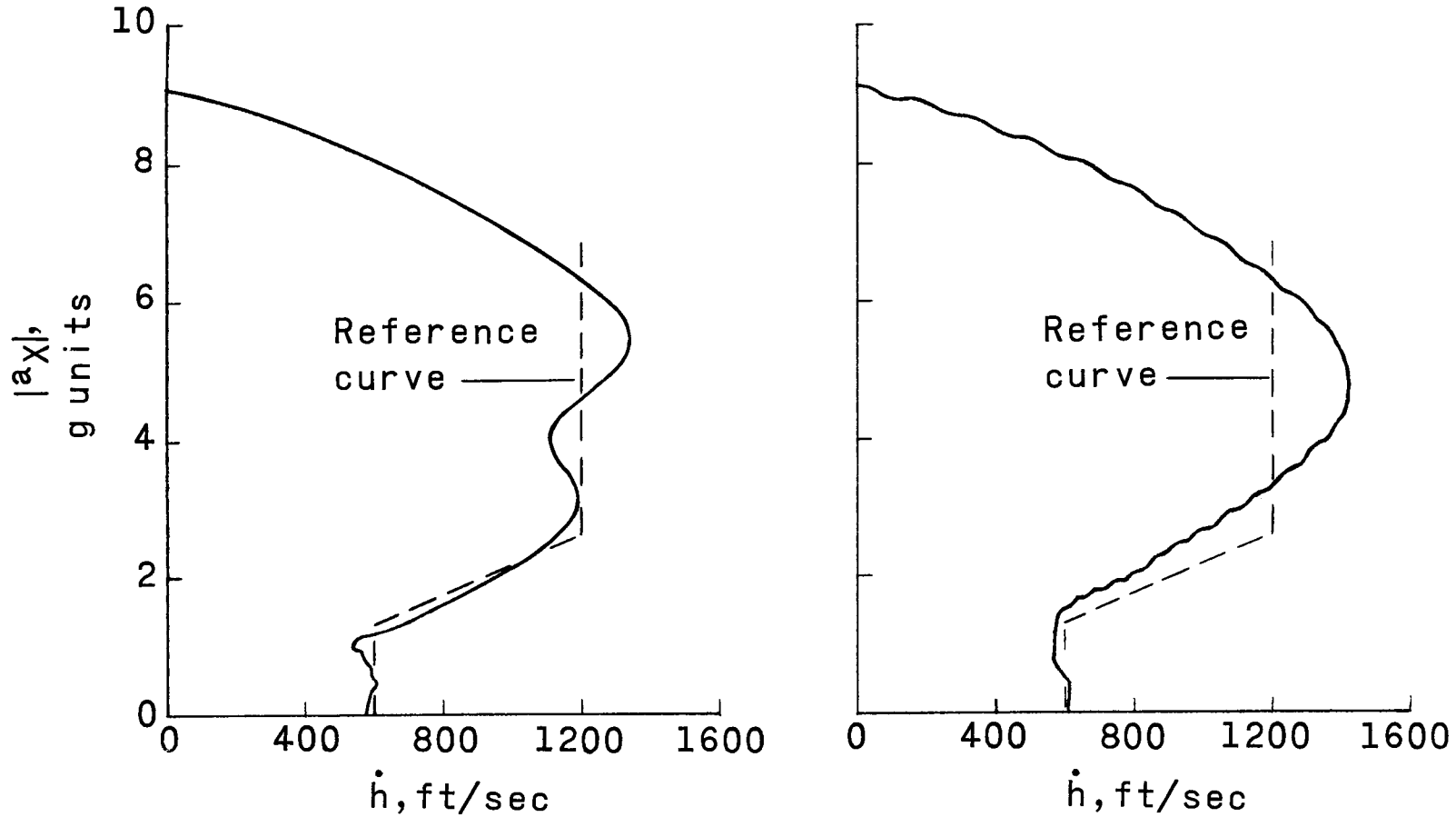

(a) Rapid rolling technique.

(b) Slow rolling technique.

Figure 6.- Effect of crossrange requirement on pilot task performance.

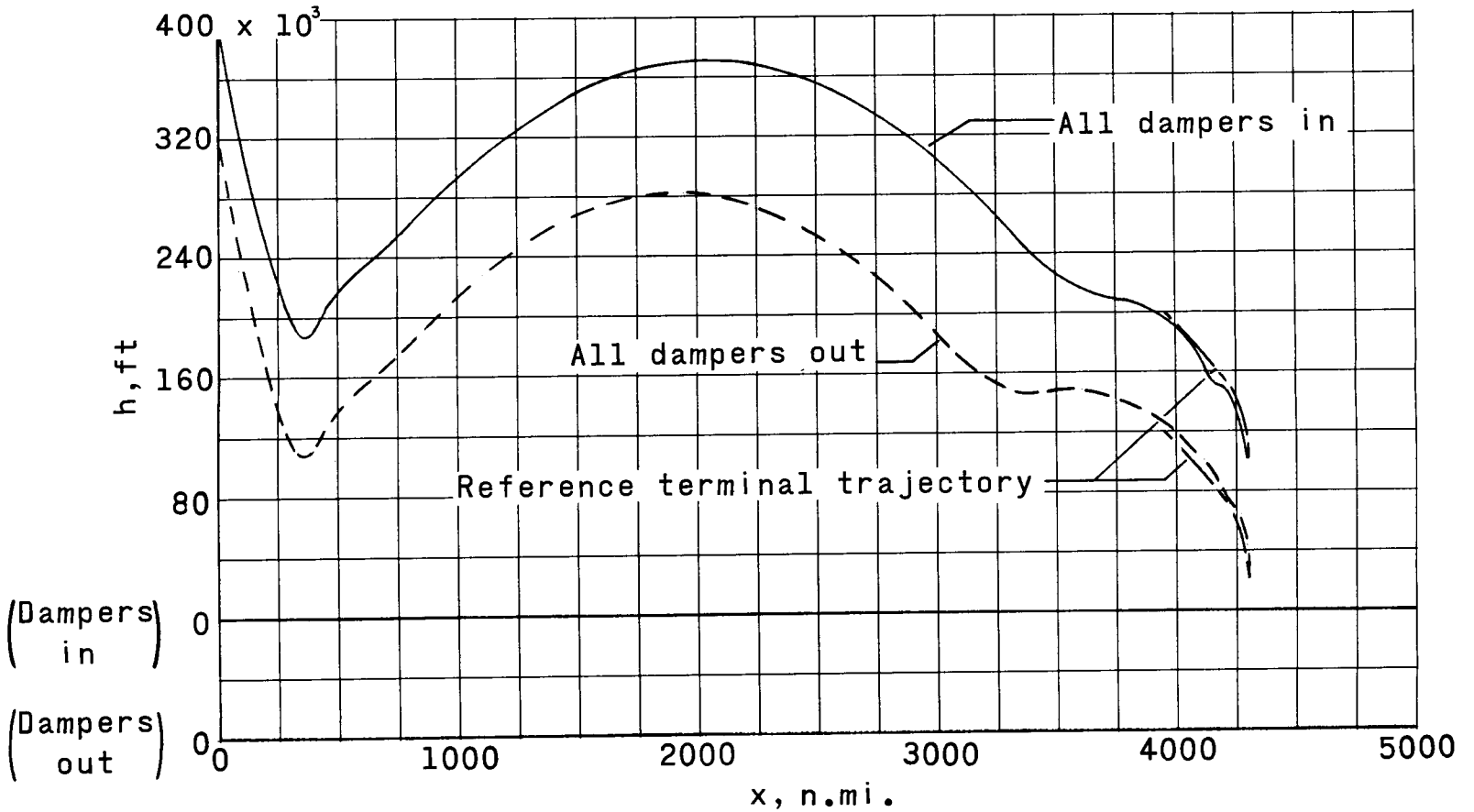

Figure 7.- Altitude—downrange-distance trajectories for long-range entries.

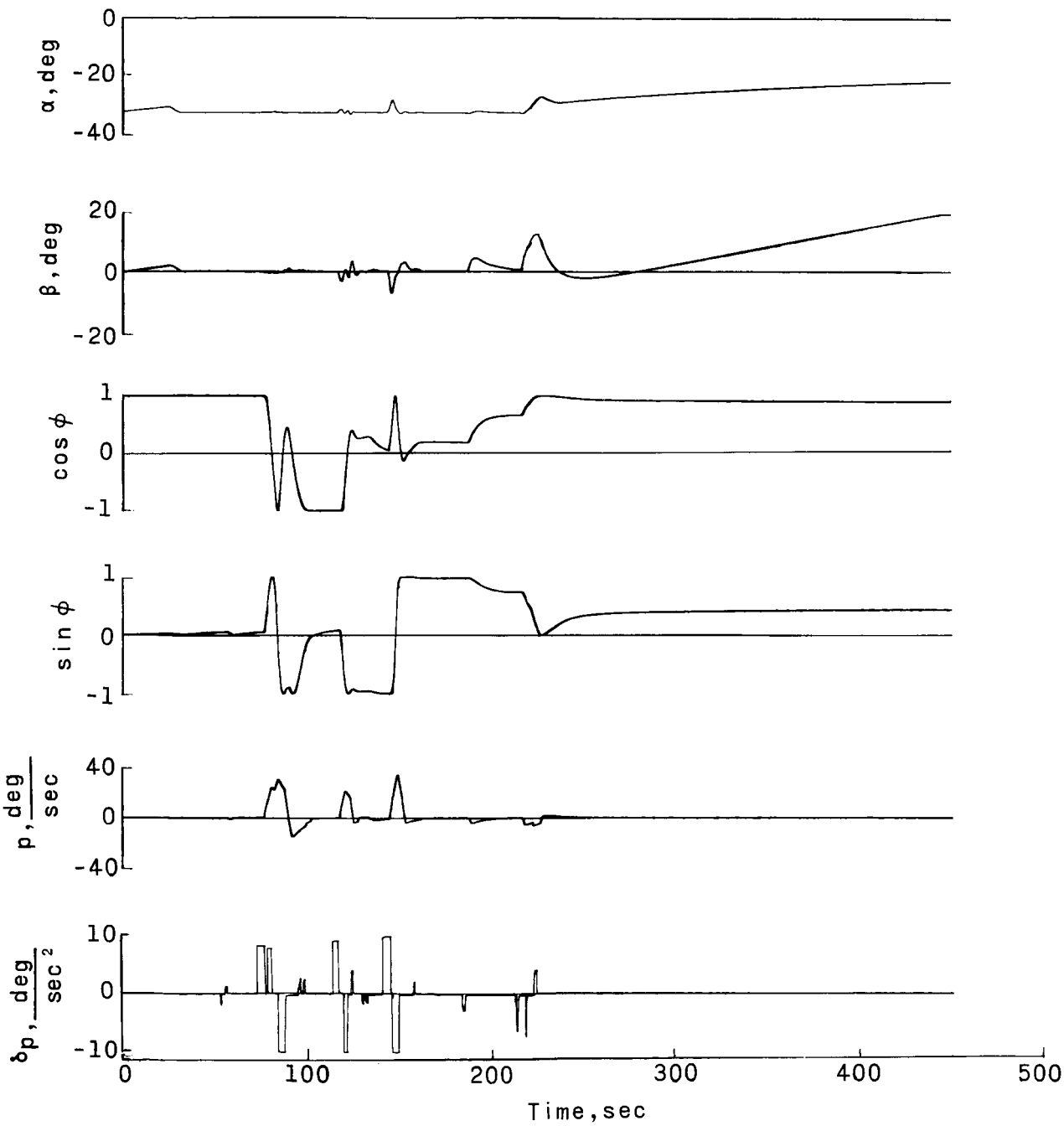

(a) Dynamic variables.

Figure 8.- Time histories of long-range entry with all dampers in.

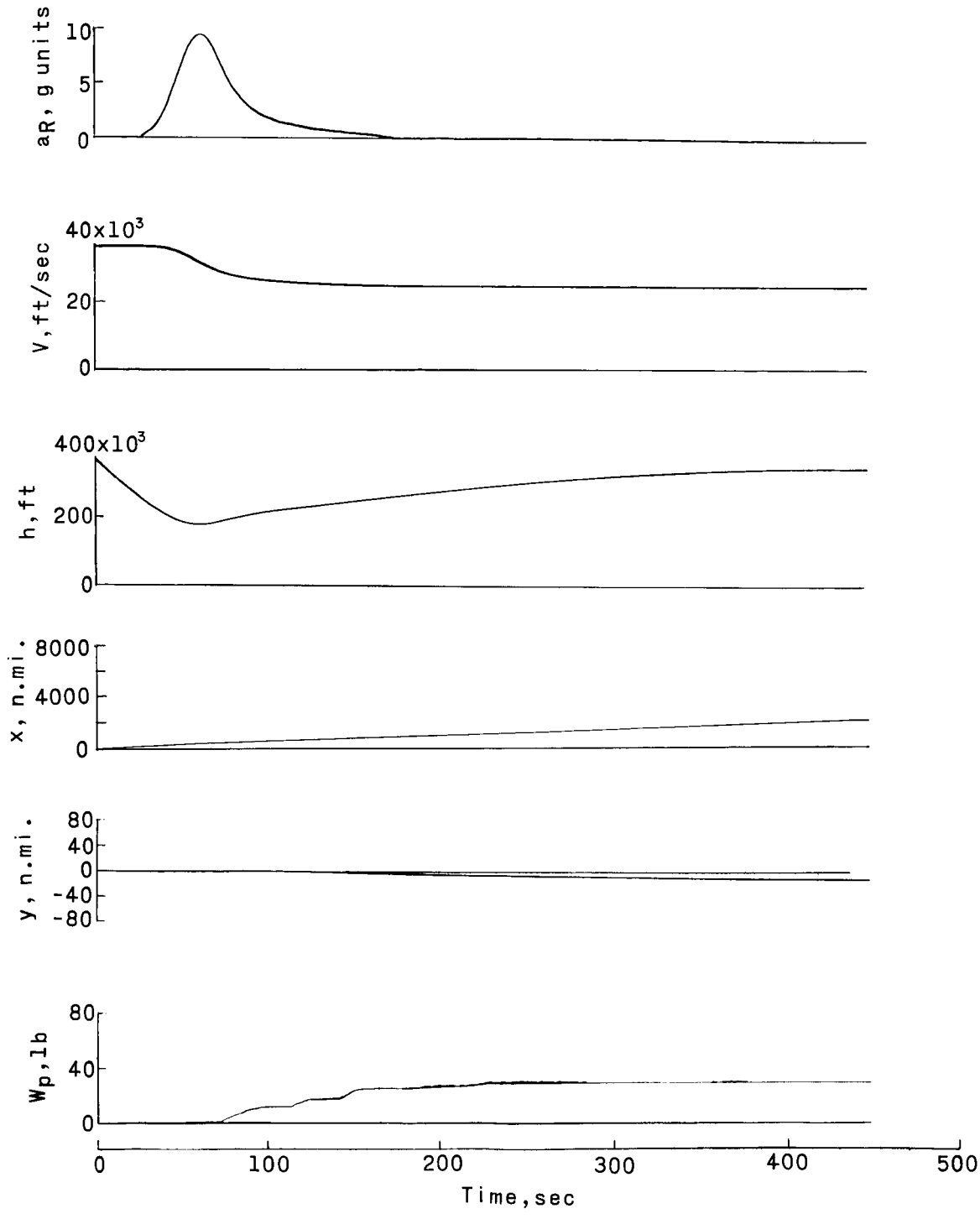

(b) Trajectory variables.

Figure 8.- Concluded.

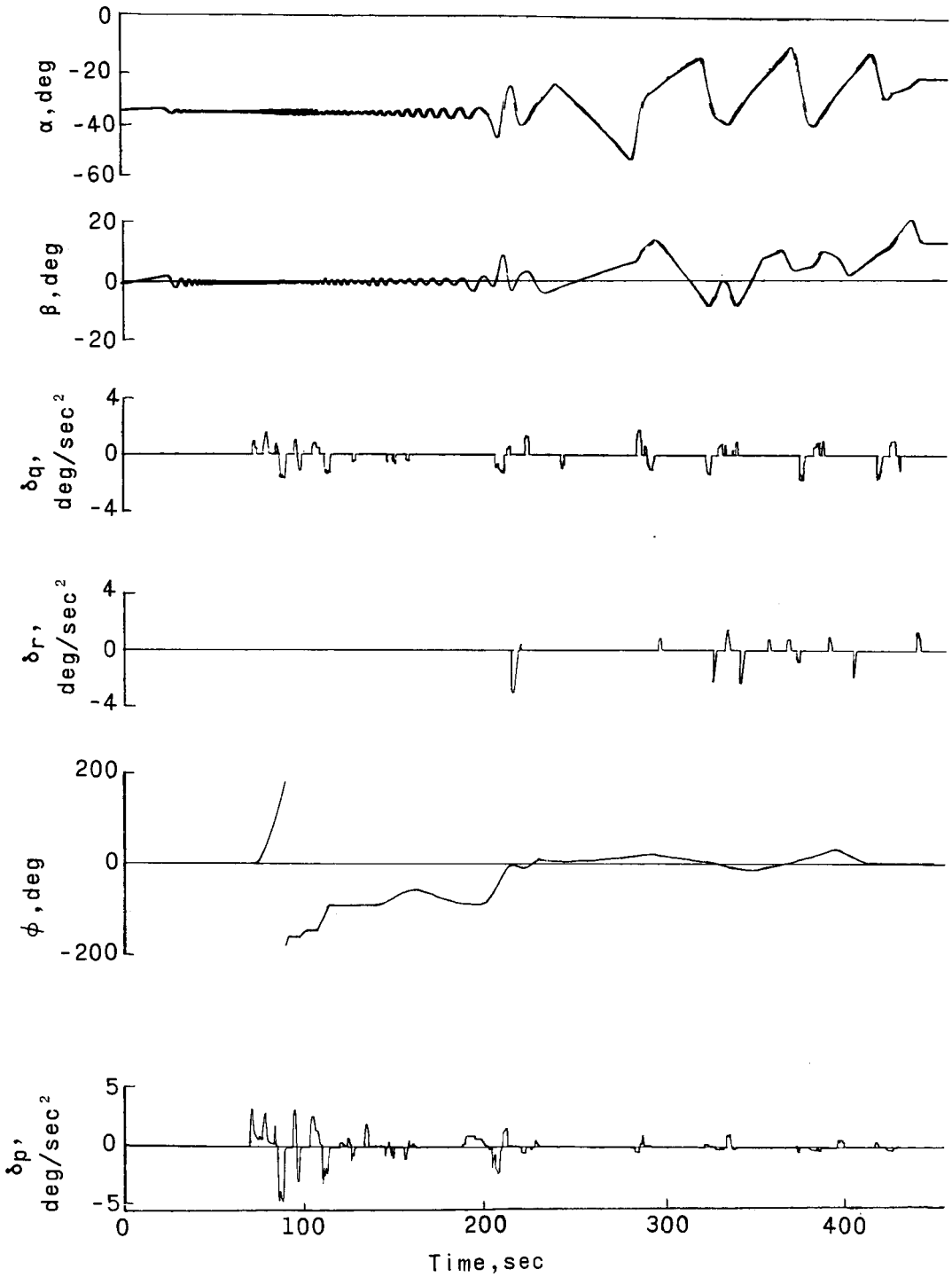

(a) Dynamic variables, $t < 450$.

Figure 9.- Time histories of long-range entry with all dampers out.

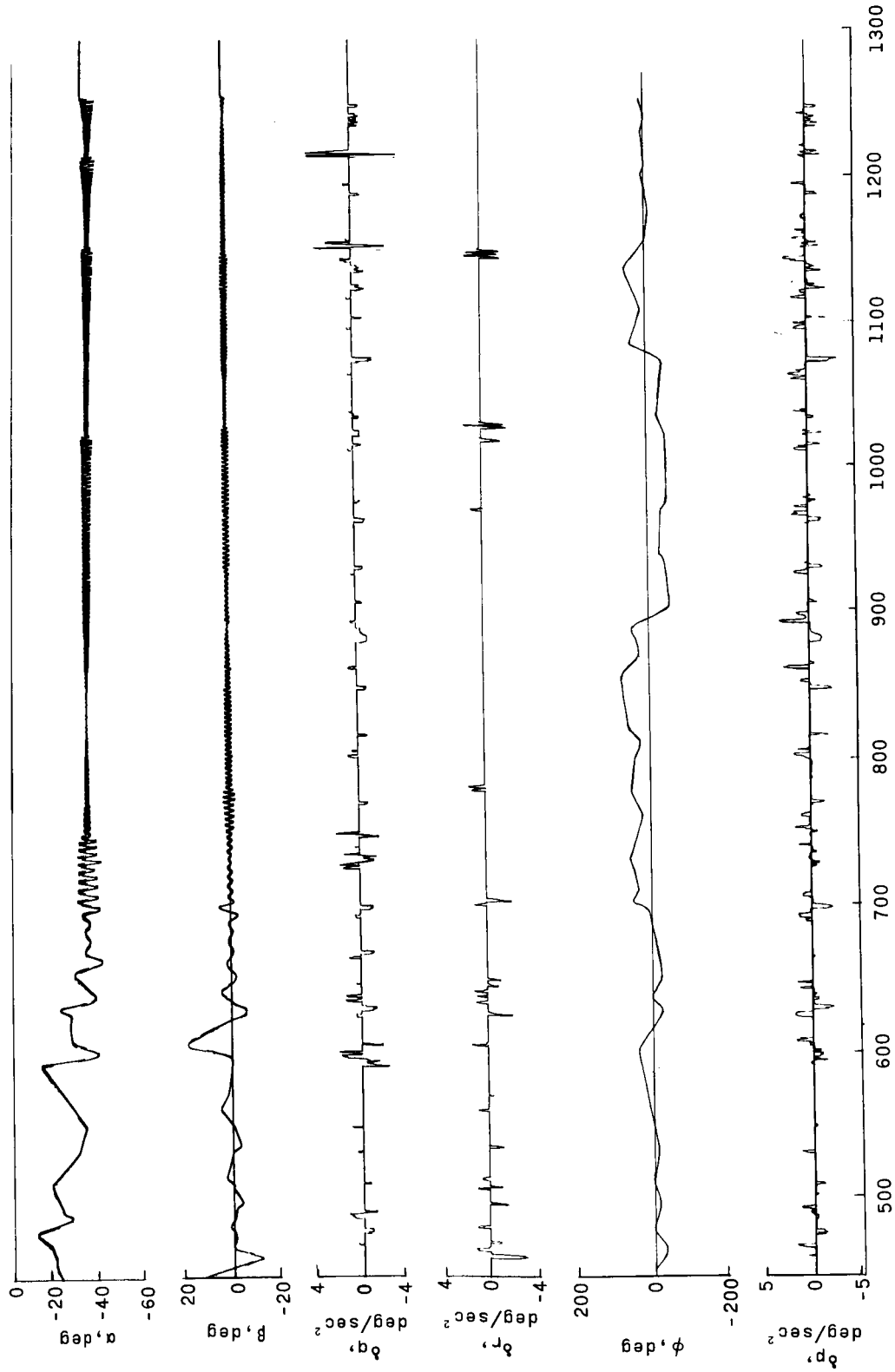

(b) Dynamic variables, $t > 450$.

Figure 9.- Continued.

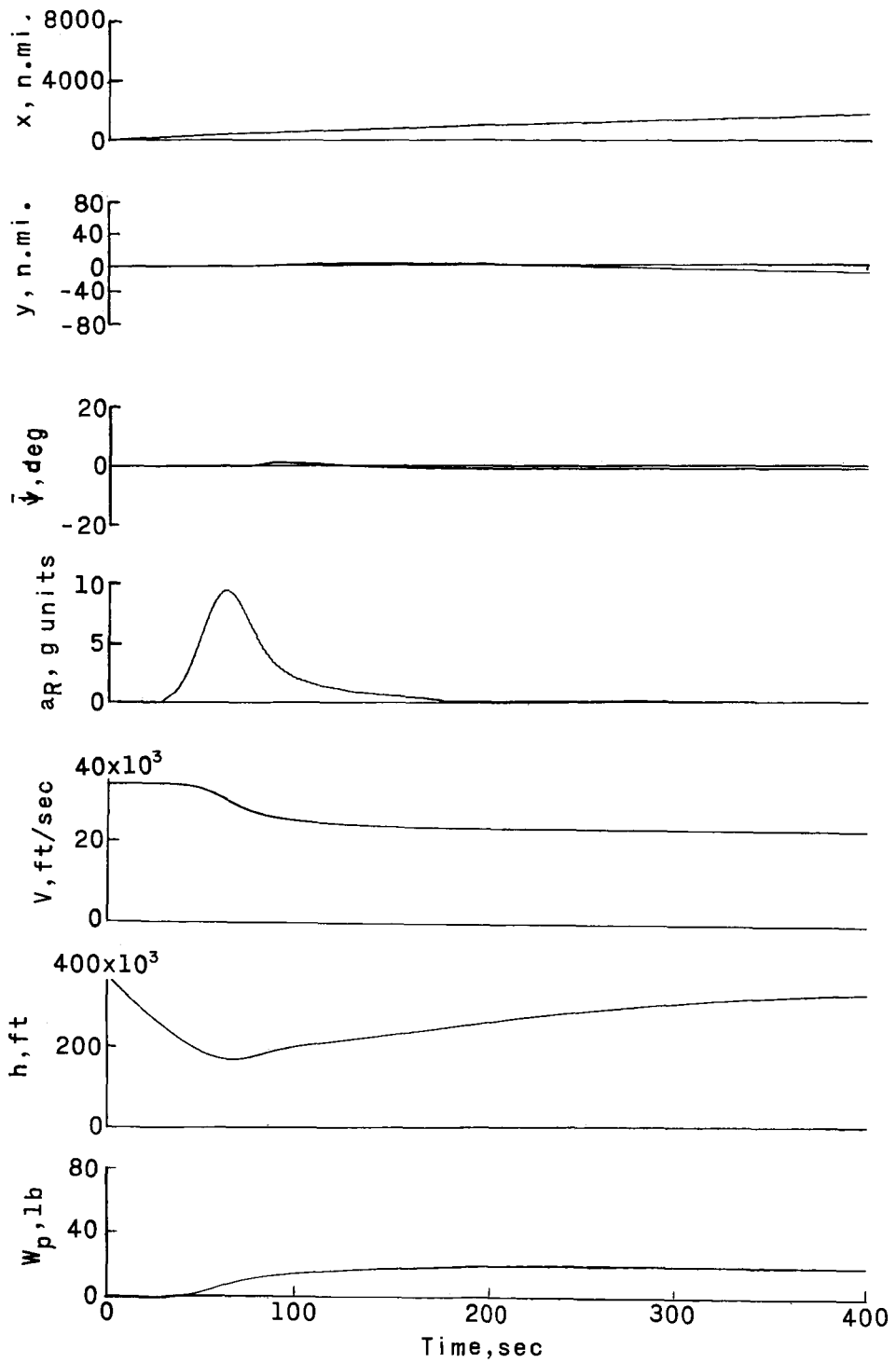

(c) Trajectory variables, $t < 450$.

Figure 9.- Continued.

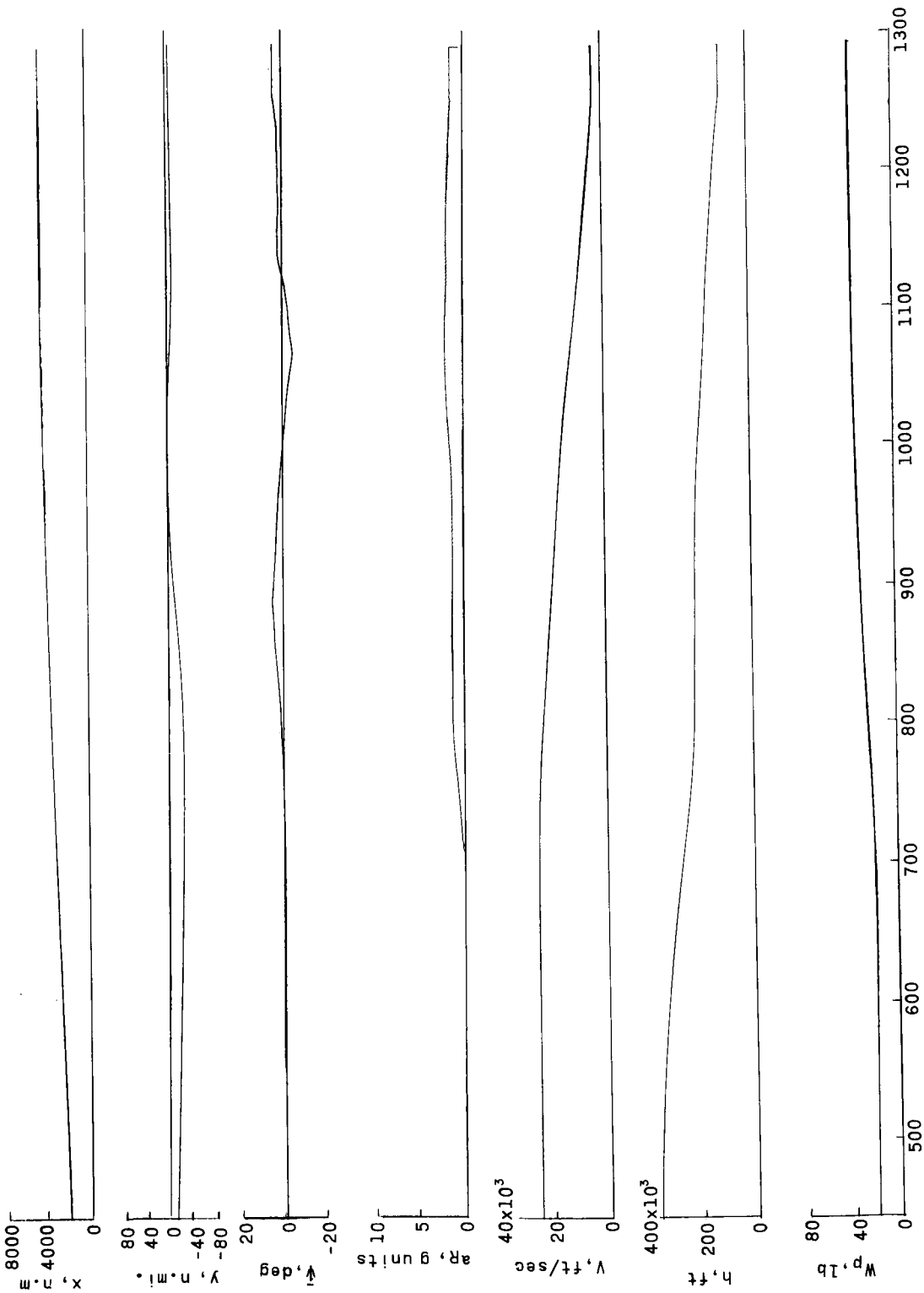

(d) Trajectory variables, $t > 450$.

Figure 9.- Concluded.

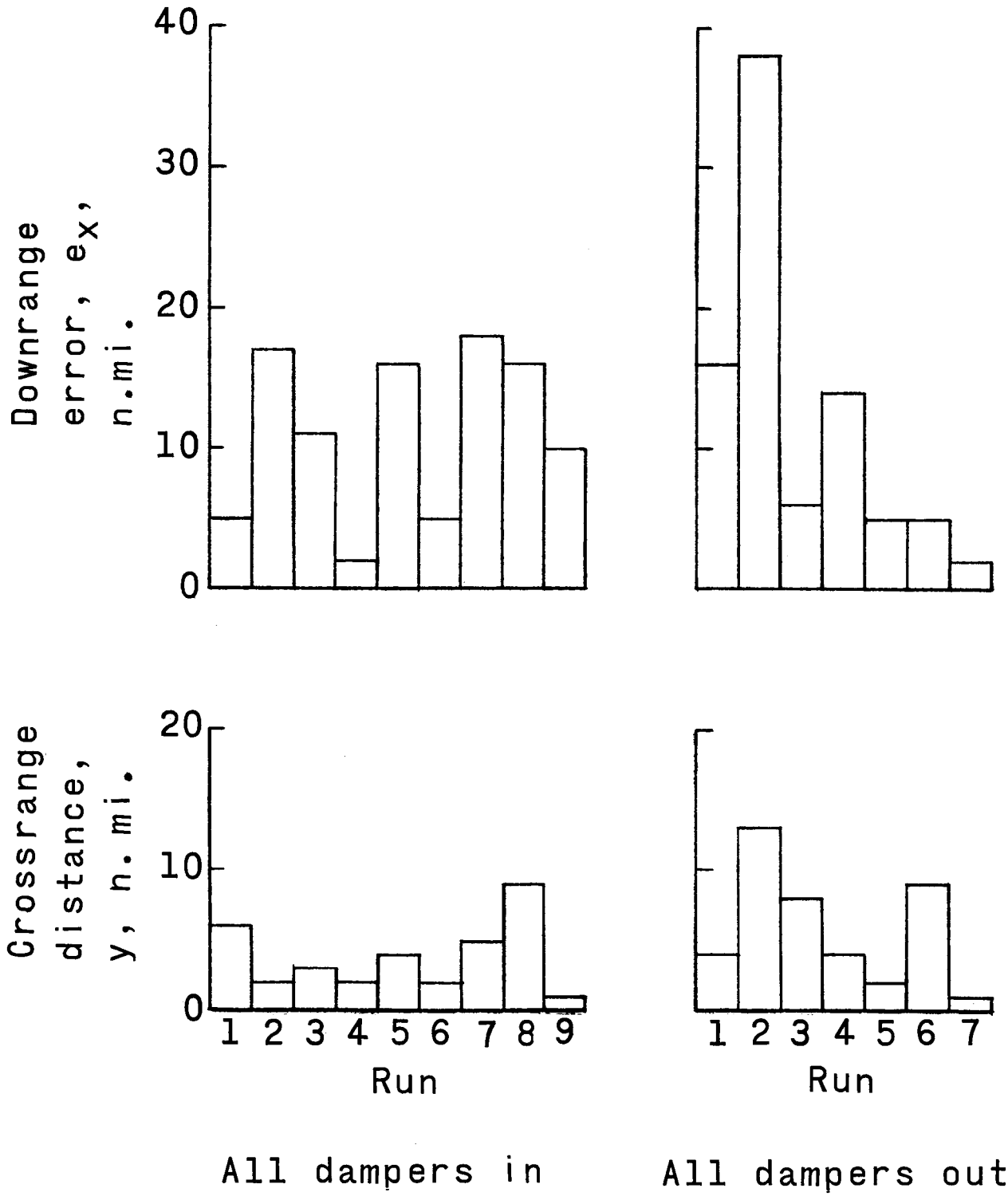

Figure 10.- Range errors and propellant consumption in long-range entries.

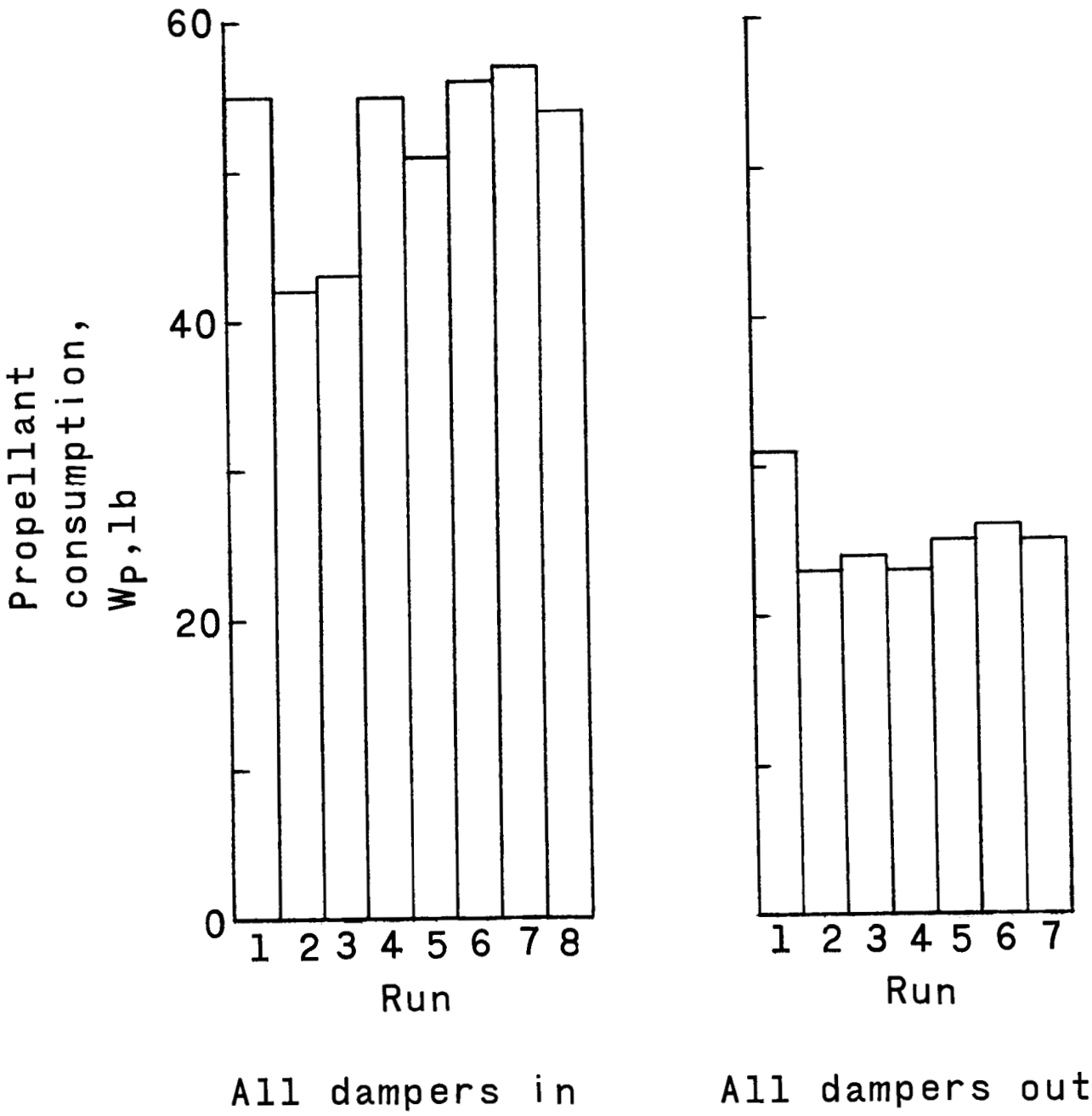

Figure 10.- Concluded.

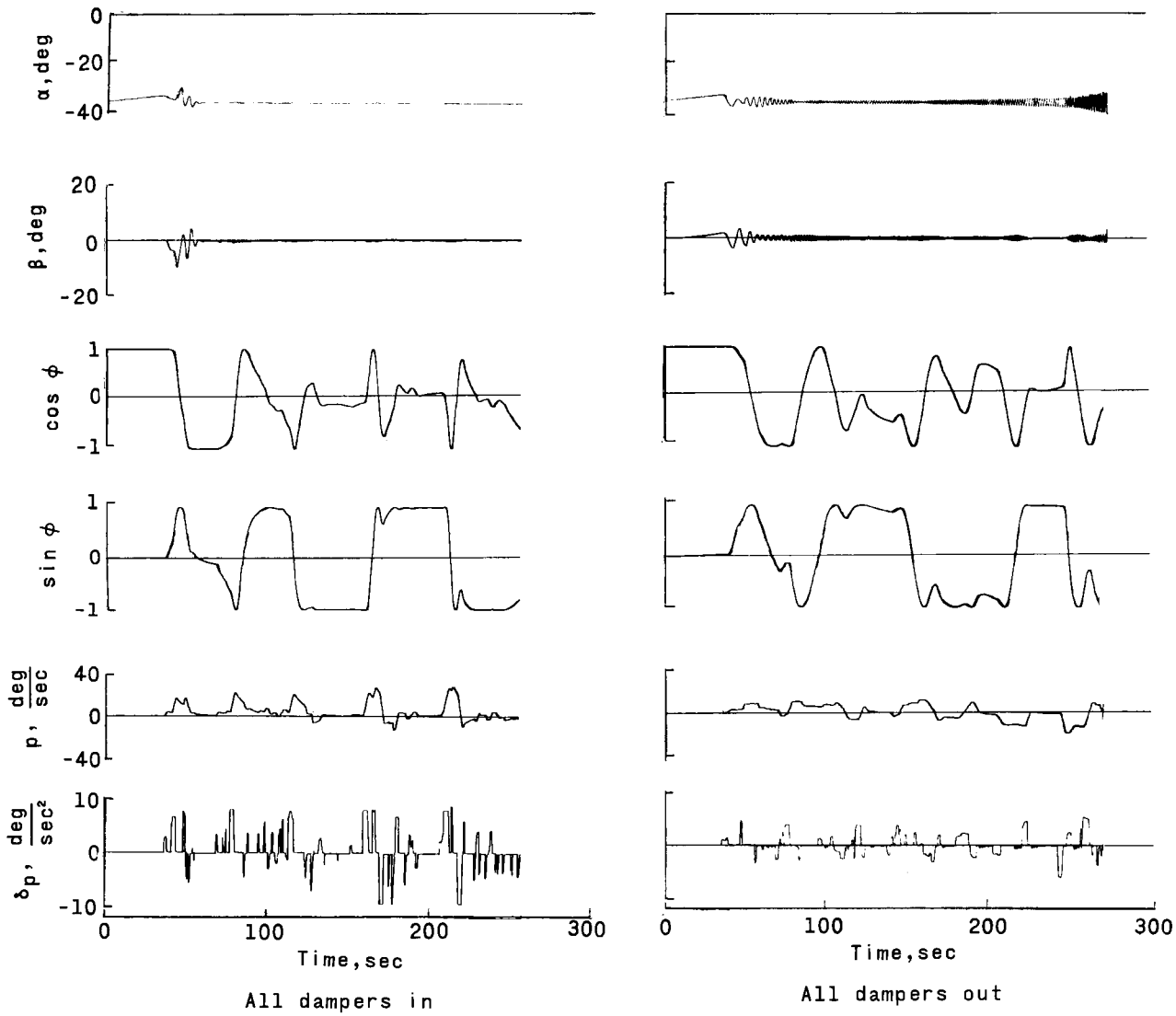

(a) Dynamic variables.

Figure 11.- Time histories of short-range entries.

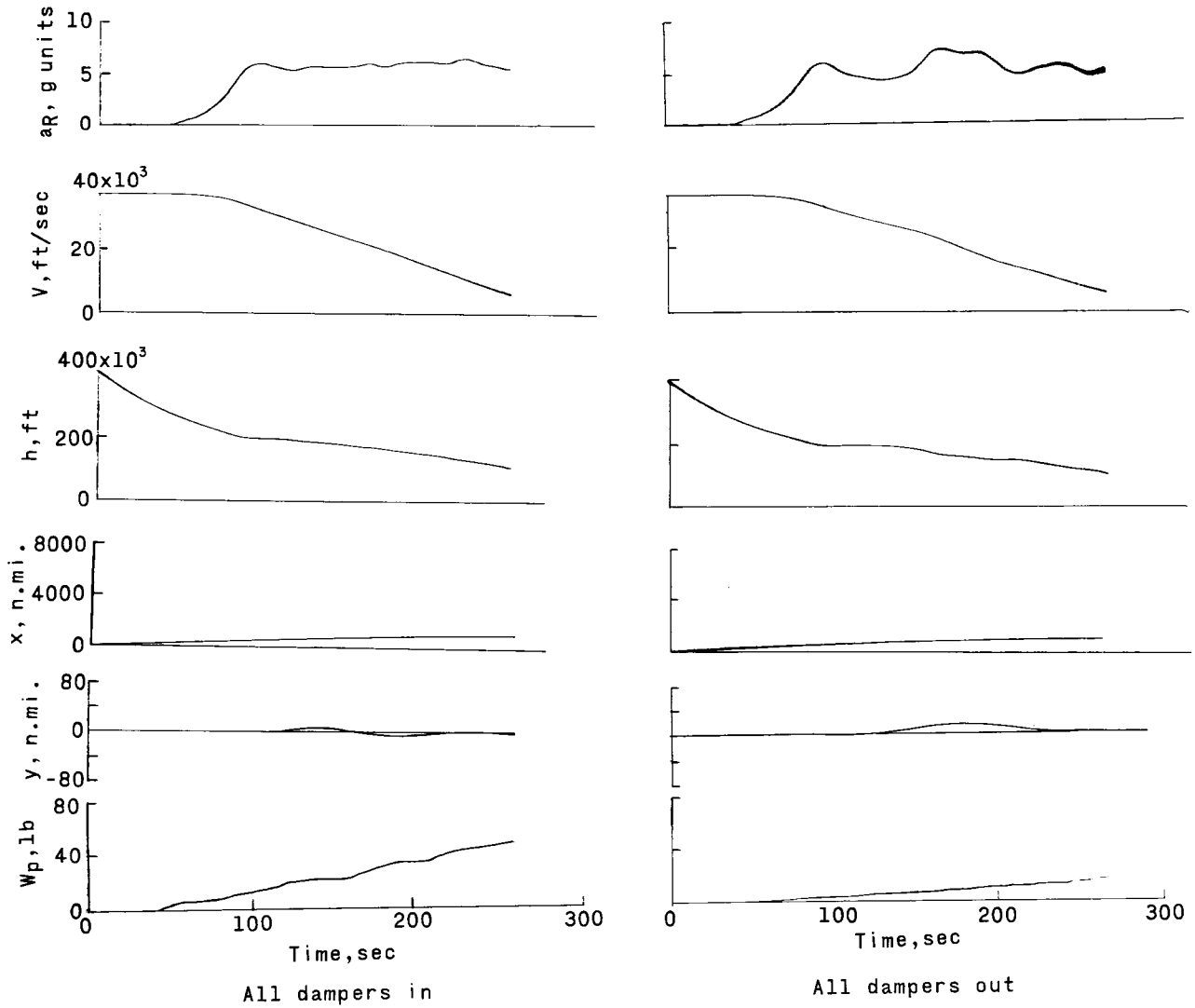

(b) Trajectory variables.

Figure 11.- Concluded.

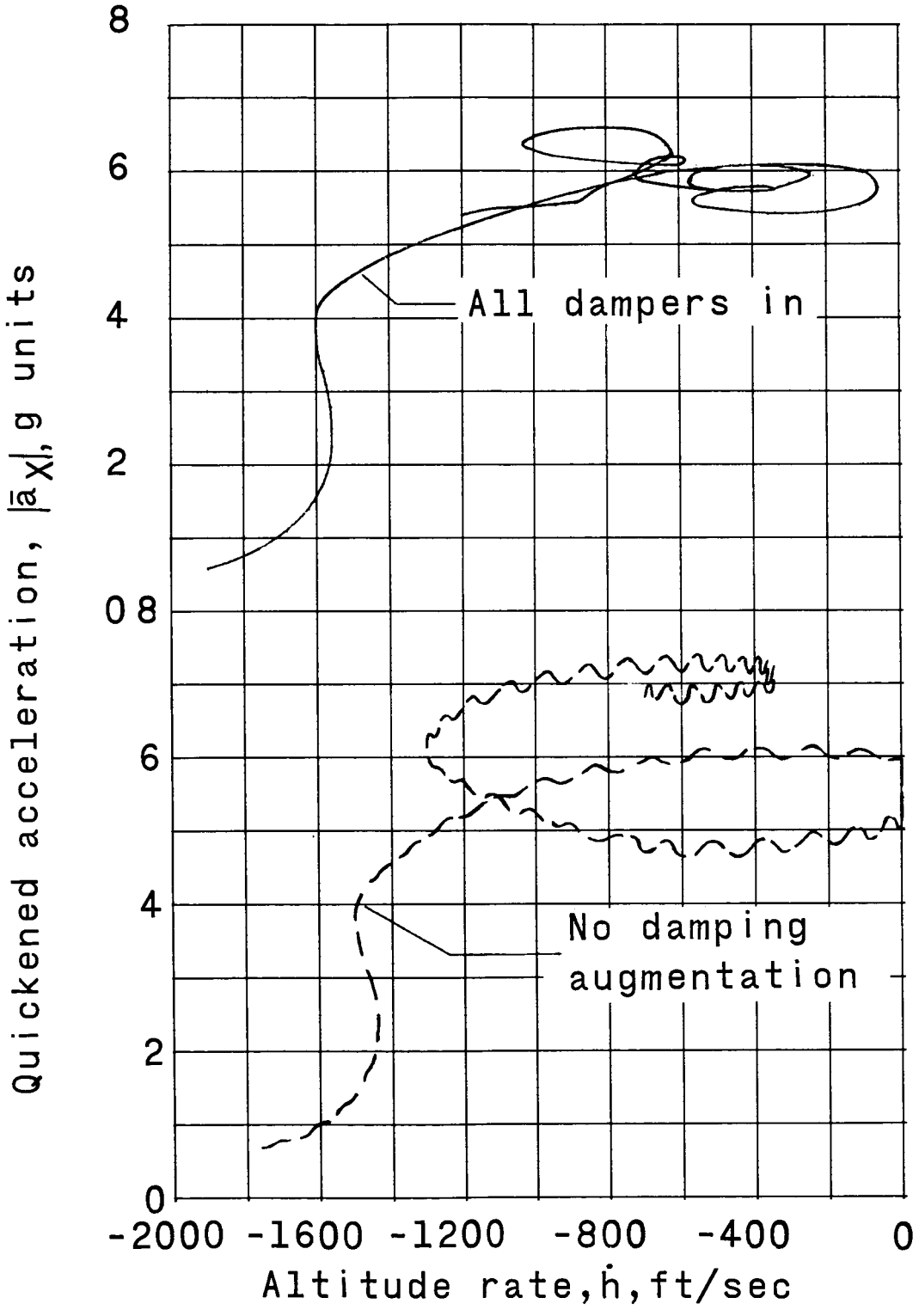

Figure 12.- Recording of oscilloscope presentation during short-range entries.

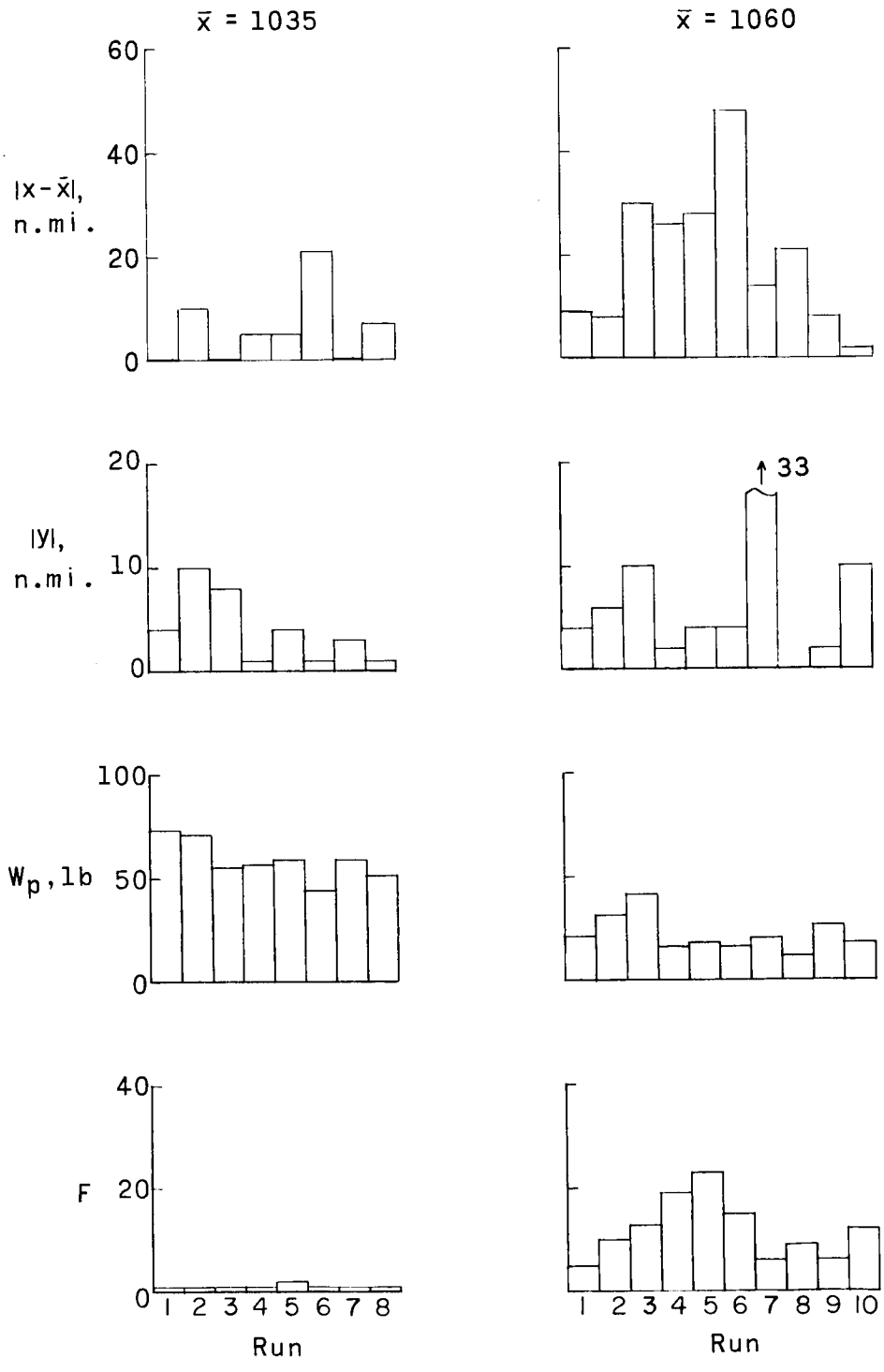

(a) All dampers in.

(b) All dampers out.

Figure 13.- Effect of damping augmentation on short-range entries. $\gamma_o = -5\frac{1}{2}^\circ$.

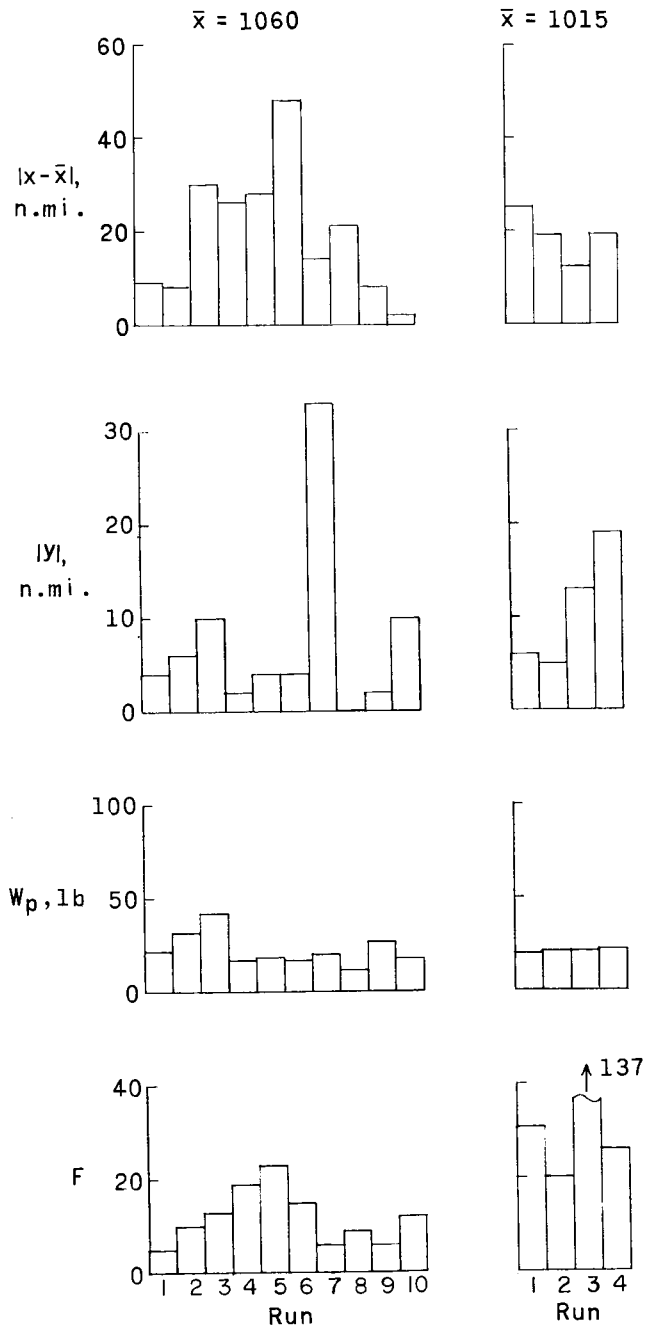

(a) Composite display of bank angle, quickened acceleration, and altitude rate.

(b) Individual meter displays.

Figure 14.- Effect of display scanning on performing short-range entries with all dampers out. $\gamma_o = -5\frac{1}{2}^\circ$.

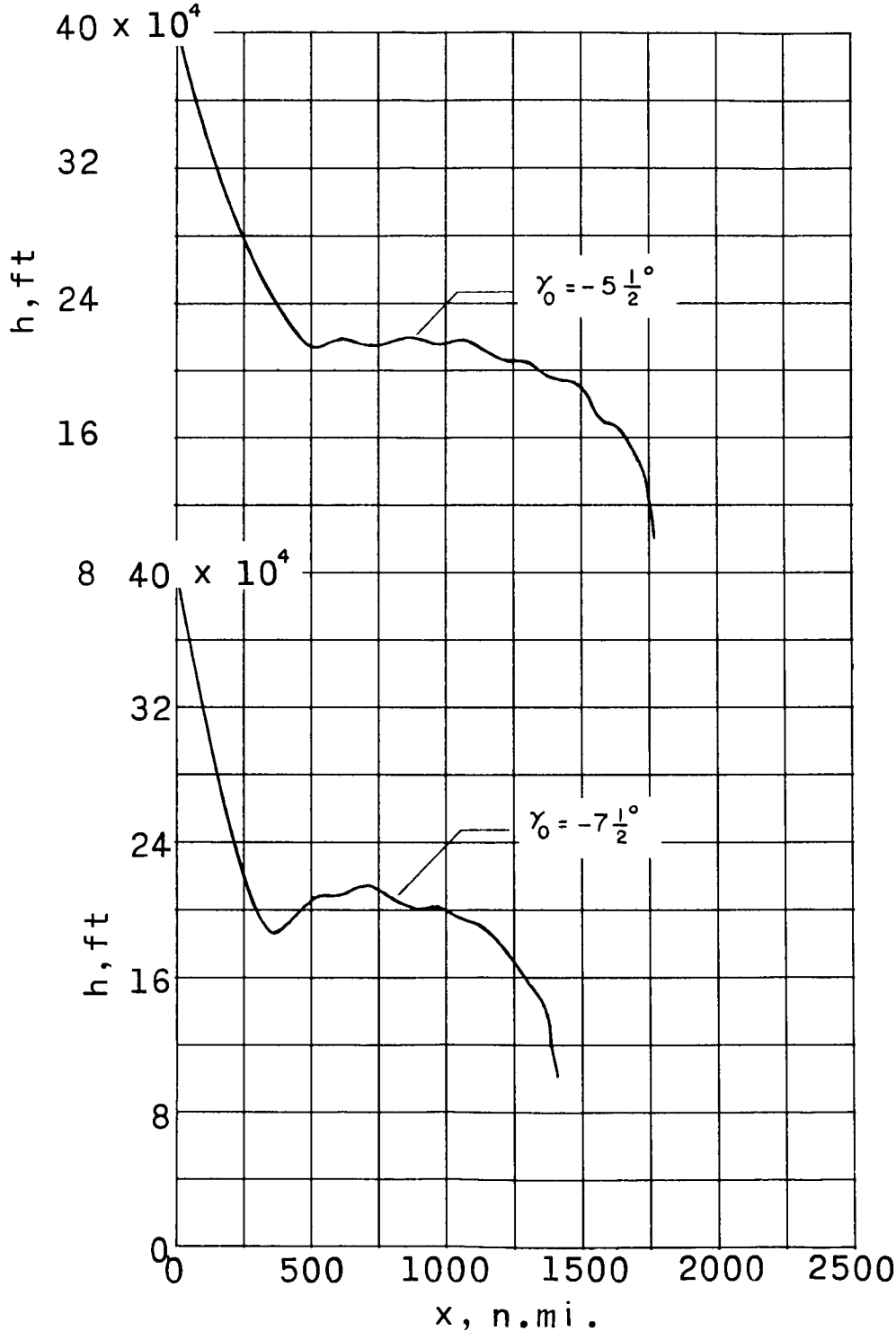

Figure 15.- Effect of entry angle on trajectories performed with instrument displays of only bank angle and acceleration.

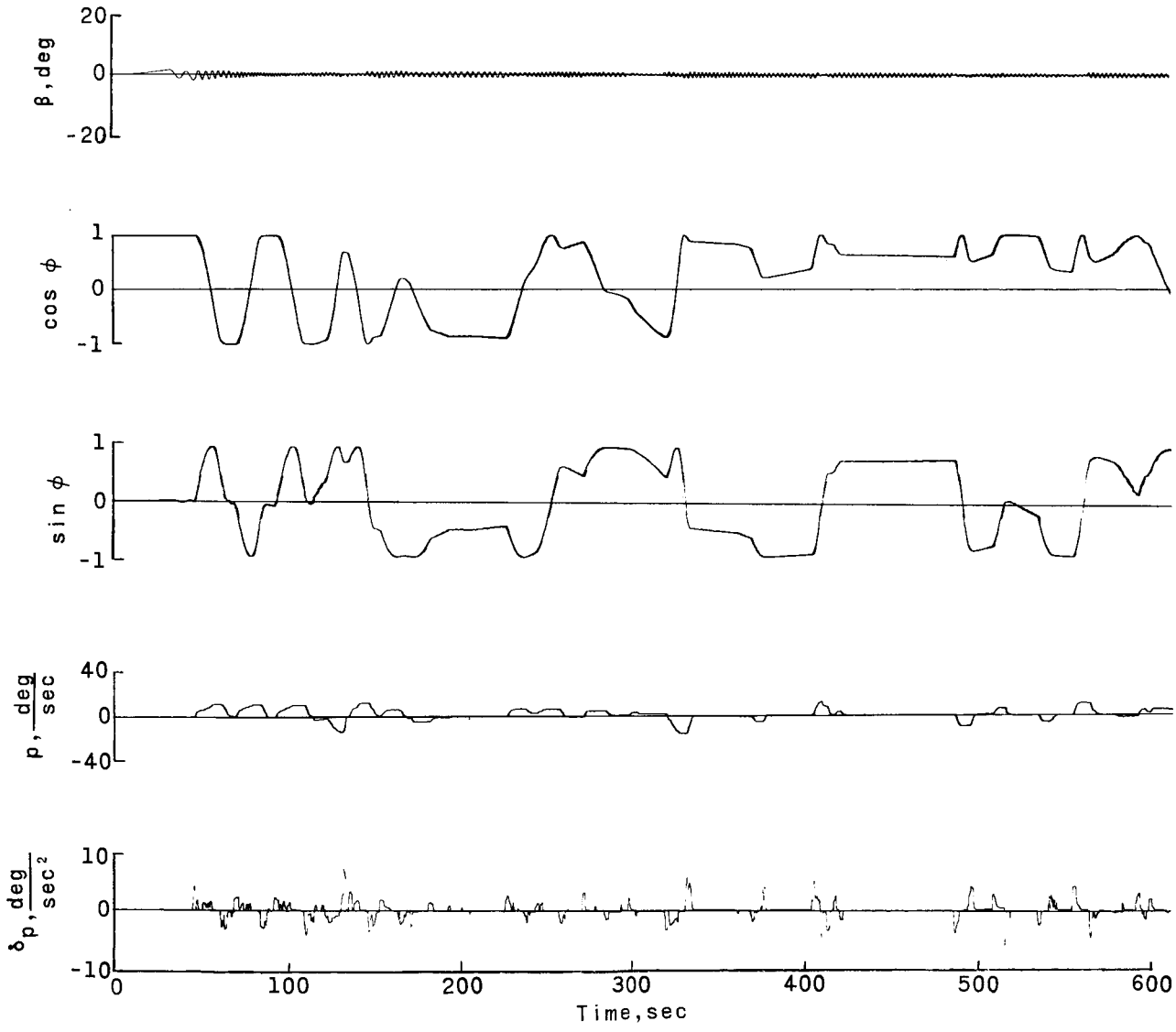

(a) Dynamic variables.

Figure 16.- Time histories of minimum-display entry with pitch damping augmentation only.

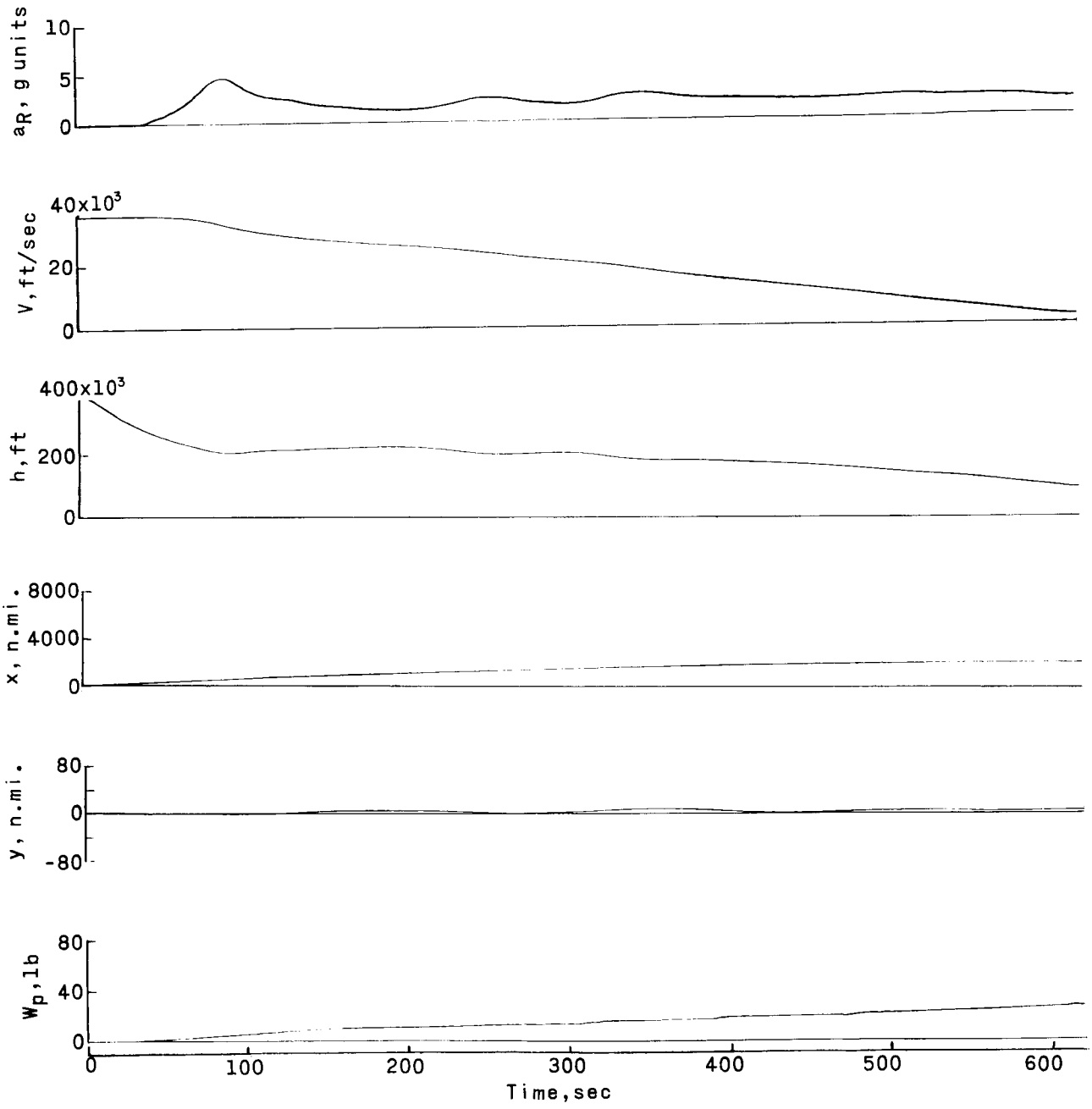

(b) Trajectory variables.

Figure 16.- Concluded.

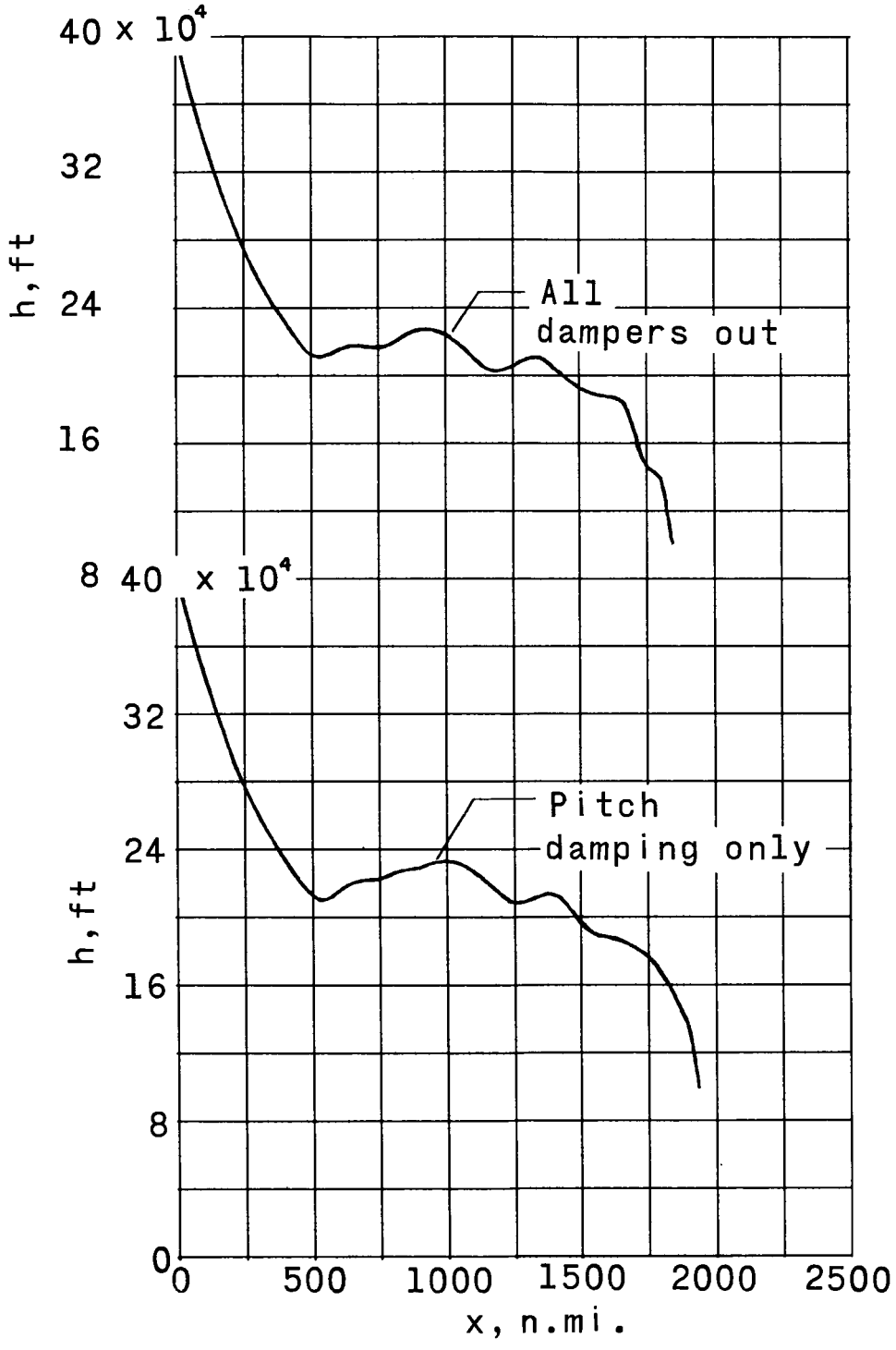

Figure 17.- Effect of damping augmentation on trajectories of minimum-display entries. $\gamma_o = -5\frac{1}{2}^\circ$.

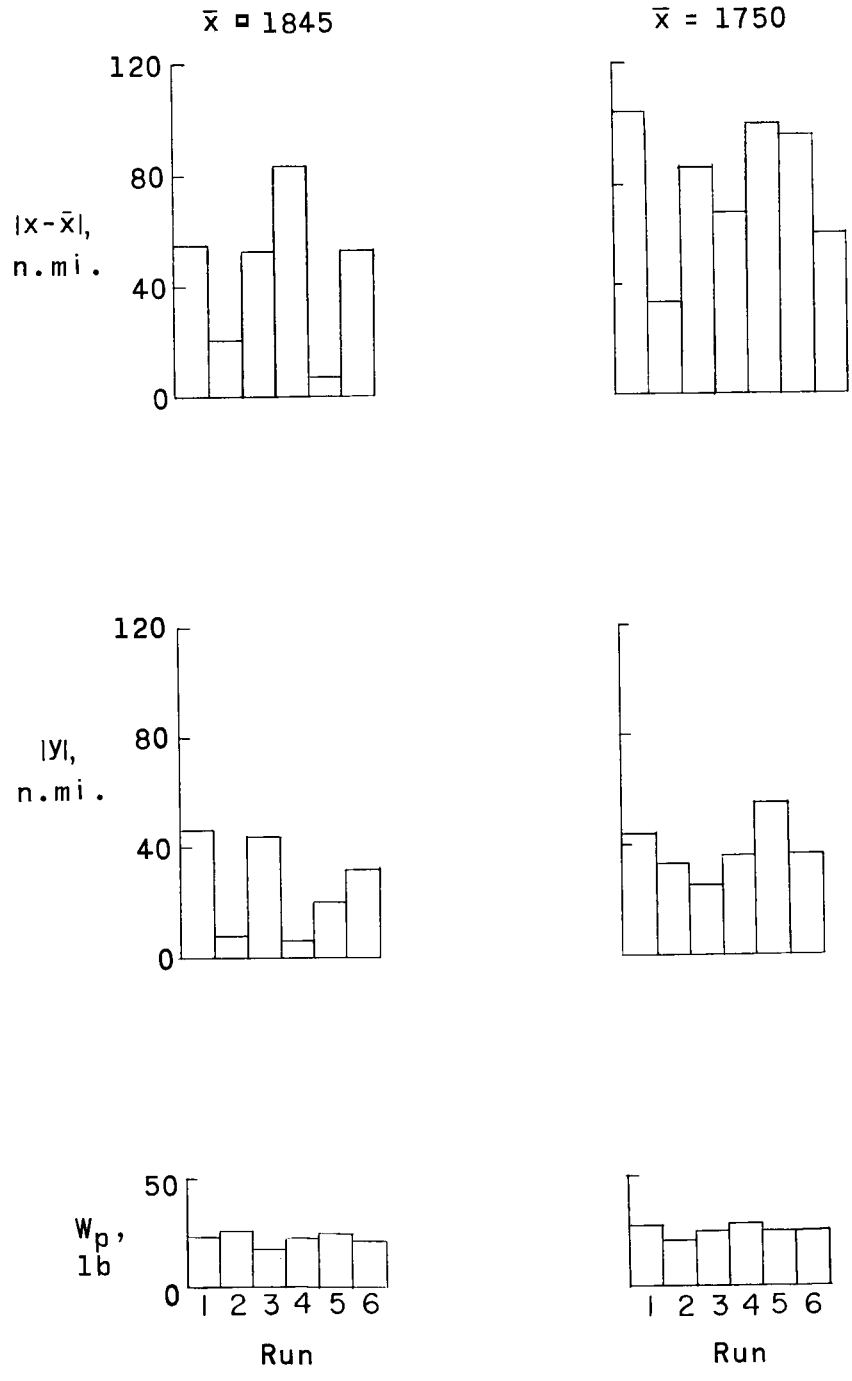

(a) Pitch damping only.

(b) All dampers out.

Figure 18.- Effect of damping augmentation on entries performed with instrument displays of only bank angle and acceleration. $\gamma_o = -5\frac{1}{2}^\circ$.

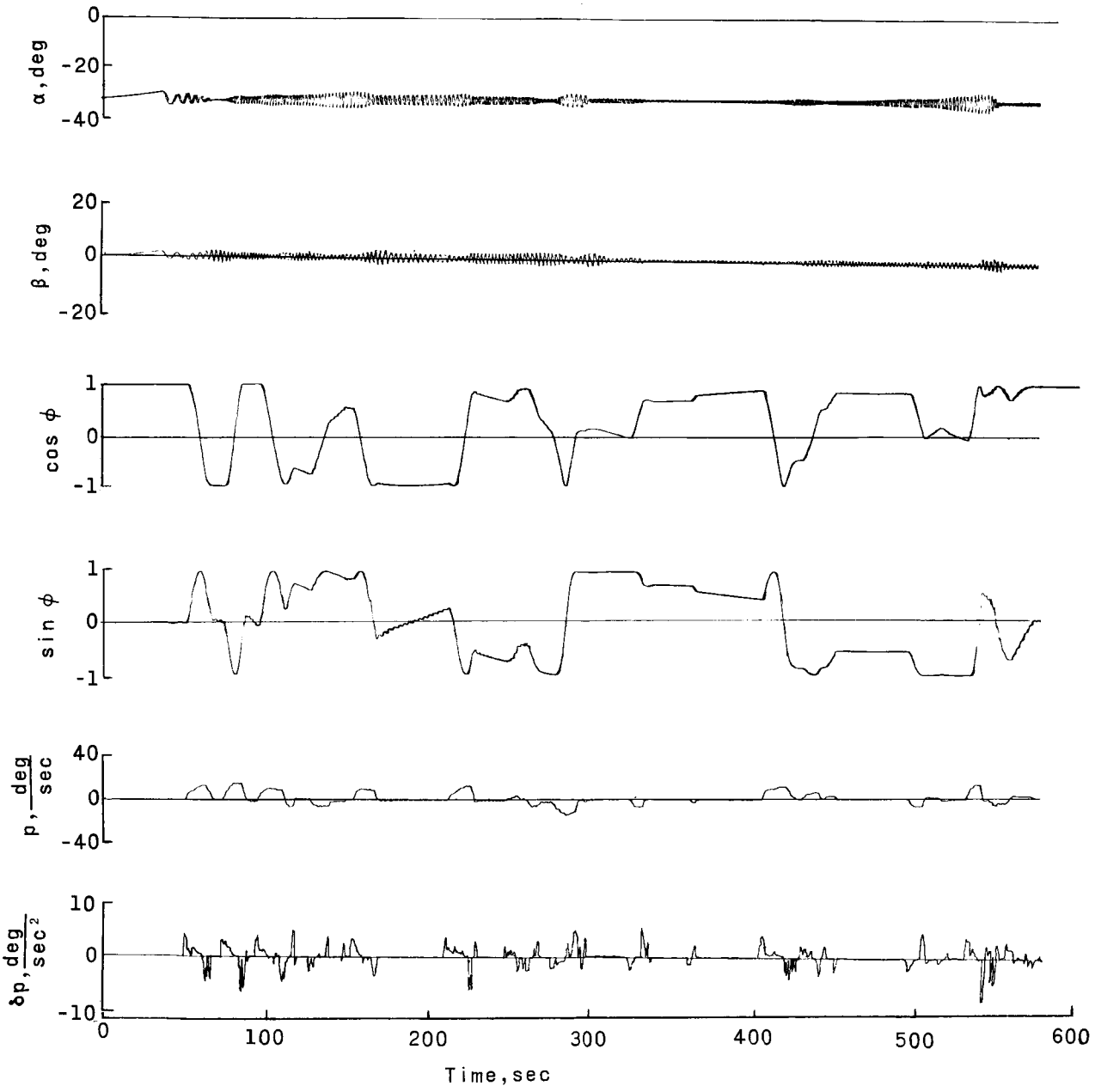

(a) Dynamic variables.

Figure 19.- Time histories of minimum-display entry with no damping augmentation.

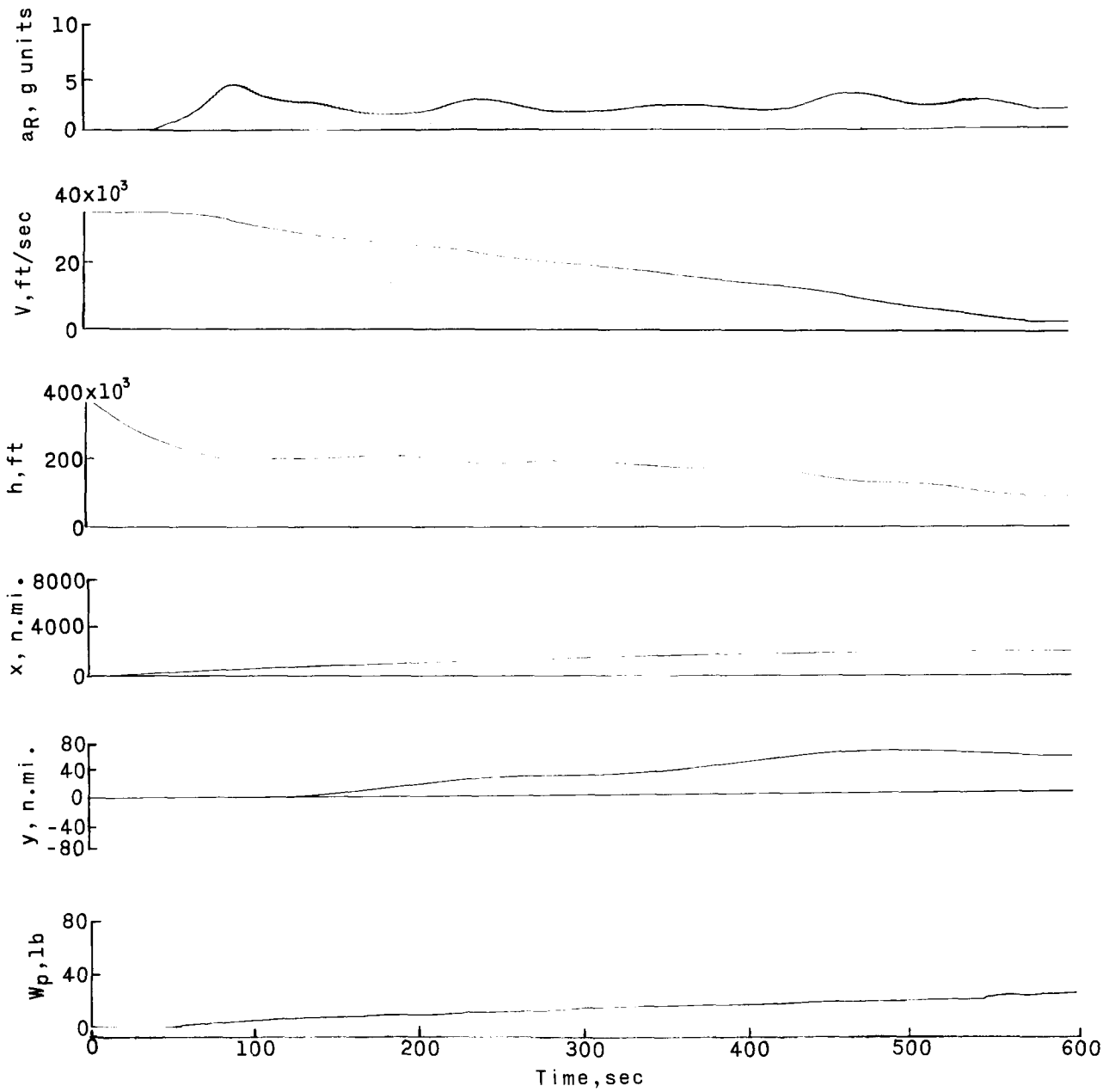

(b) Trajectory variables.

Figure 19.- Concluded.

NASA-Langley, 1965 L-4045